

## Multichannel spectrophotometry and the luminosities of white dwarfs

Jesse L. Greenstein

Hale Observatories, California Institute of Technology, Carnegie Institution of Washington, Pasadena, California 91125

(Received 19 February 1976)

Multichannel observations permit classification of the degenerate stars, and the colors are highly correlated with their luminosities. From about 5000 to 50 000°K the color-magnitude diagram can be explained by a constant mean radius  $0.0109 R_{\odot}$  from theoretical calibration of the colors. The most useful color is that from  $1/\lambda = 2.12$  to  $1.25 \mu^{-1}$ ; the scatter in  $M_{1.85}$  from good parallaxes is less than  $\pm 0.44$  mag. Three different colors predict  $M_{1.85}$  within  $\pm 0.17$ . Table II contains the MC data on 181 stars; Table III contains 72 stars, of which 67 have directly determined  $M_V$ . Table V contains predicted parallaxes (many of them easily measurable) and space motions. These degenerate stars have intermediate velocities (old disk and Population I) and only 3% have halo motions. The median luminosity for 178 stars is  $\pm 12.2$ ; few are very bright ( $< 10$ ) and few are faint ( $> 15$ ). Thirty stars without parallax have been added with  $M > 13$ , i.e., cooler than 7000°K.

RAPID production of good parallaxes for faint stars has made possible recently a straightforward study of the color-luminosity relation for white dwarfs. Earlier studies were based on then available parallaxes, cluster or binary star membership, and broad-band photometry. Astrophysical interpretation of such colors, Strömgren photometry, or scans, together with interpretation of line profiles lead to temperature, surface gravity, and radius. In this paper, multichannel photometry at the 5.1-m Hale reflector is combined with available parallaxes to obtain various color-luminosity relations. These are used to obtain the mean radius. They also provide interpolation formulae to predict luminosity and space motion for a larger number of degenerate stars, for which parallaxes are lacking. For these we can also predict parallaxes which will be worth measurement. It is a pleasure to express my indebtedness, as an astrophysicist, to those whose careful astrometric work made this straightforward approach possible. Not only the number, but the quality of parallaxes have greatly improved. In Eggen and Greenstein (1965) there are 19 white dwarfs listed with useful parallax. Of them, two are too far south for any further observation (EG 82, 165), and one (EG 96) is not degenerate. In this paper there are 67 stars with relatively reliable luminosities, of which only a few are calibrated by a common proper companion.

This is the first in a series of papers employing multichannel (MC) photometry to study proper motion stars. Oke's (1974) paper describes his measurement of  $AB$  monochromatic magnitudes for white dwarfs.

$$AB = -2.5 \log f_{\nu} - 48.60. \quad (1)$$

Here  $f_{\nu}$  is the flux in ergs/sec/cm<sup>2</sup>/Hz based on the Oke and Schild (1970) calibration of  $\alpha$  Lyrae. Oke finds that the MC does not give absolute photometry of the same quality as broad- or narrow-band photoelectric photometry, because a standard extinction table is used in the computer reduction. The intermediate standards are five well-calibrated sdG stars, which are nearly line free. The colors obtained are better than the absolute photometry. Two problems

specifically affect the colors of white dwarfs. The breadth of the hydrogen lines ( $\approx 70 \text{ \AA}$ ) and the resolution I used (normally  $40 \text{ \AA}$  at  $\lambda < 5700$ ,  $80 \text{ \AA}$  at  $\lambda > 5700$ ) combine to depress the observed continuum at  $\lambda < 4340$  in DA stars, well before the Balmer limit. There is a residual uncertainty in the absolute calibration centered on  $\lambda 3880$ , and it is possible that the Balmer jump should be larger. These affect the visibility of weak Ca II lines in DA, F, or DF stars.

The observations reported here are generally based on one scan per star. The appearance of the scans is shown in Figs. 1 to 3 of Oke (1974), some at higher resolution ( $20/40 \text{ \AA}$ ), or based on more than one scan per star. My statistical errors are usually less than  $\pm 0.02$  mag, except in the infrared or for very faint stars. Quality and resolution are graded A-C in the data table, but the significant errors largely arise from the uncertainty in luminosity, or in line blanketing. It is difficult to present MC data in full, since there are 120 measured points. The white dwarfs have relatively simple spectra; measurement, with some smoothing, at a limited number of wavelengths, eight, is sufficient for classification and colorimetry. Information concerning these is in Table I. The full MC output will be used elsewhere, for fitting model atmospheres. We find that only a few colors are necessary for the luminosity calibration. Since the tables are machine printed, capital letters are used to name the central frequencies; a color  $G-R$  corresponds to  $m(2.12)-m(1.44)$  or

TABLE I. Monochromatic magnitudes and colors used.

$1/\lambda$ ( $\mu^{-1}$ )	Name	Color	Remarks
1.00	$I^*$	$R^*-I^*$	Useful for dM stars
1.25	$I$	$R-I$	Related to Kron broad band
1.44	$R$	$G-R$	Affected by $C_2$ in $\lambda 4670$ stars
1.52	$R^*$	$B-V$	Affected by $H\gamma$ in DA; $(B-V)_c \approx 0.94(B-V) + 0.14$
1.85	$V$		$V_c \approx V + 0.05$
2.12	$G$	$U-B$	Balmer jump; $(U-B)_c \approx 0.89(U-B) - 0.90$
2.35	$B$		
2.80	$U$		

alternatively to [2.12]–[1.44], where the frequencies are in inverse microns. The bandwidth  $\Delta\nu/\nu$  is about 1%, much less than the conventional *UBVRI* magnitudes. When the latter are referred to, the subscript *c* is used. A variety of color-luminosity diagrams were prepared ( $M_{2.80}$ ,  $M_{2.35}$ ,  $M_{1.25}$ ,  $M_{1.00}$ ) but only those at  $1/\lambda = 1.85$ , i.e.,  $M_V$ , or  $M_{1.85}$ , are presented here. The transformation to the broad-band  $M_{V_c}$  is simple, i.e.,  $V_c = V + 0.05$ . The extra information on luminosity the other diagrams contain is not large, because of the relatively smooth white dwarf continua. This is clearly not true for the dM stars with strong TiO bands.

#### I. NOMENCLATURE, CHARTS, SOURCES OF PARALLAX

I have used Oke's 37 degenerate stars in my Table II which contains 150 further degenerate or probably degenerate stars. For some of these, brief data appear in my series of nine papers on degenerate stars; the bibliography and numbering are in Greenstein (1974, 1975). For simplicity I retain the numeration as an EG series, although only the first three papers (through EG 202) were published with Eggen and stars after EG 266 were given Gr numbers. The heading EG is to be understood as an EG or Gr number; Eggen is not responsible for any errors in data subsequent to EG 202. An effort has been made to systematize nomenclature by using the G (Lowell Observatory) designation wherever a Lowell position and chart exist. [See Giclas, Burnham, and Thomas (1971) for northern stars and various *Lowell Bulletins* for southern.] Next, the Gliese (1969) catalog numbers were used, since broad-band colors, parallax, and motion and other designations are included; many of these GL stars are relatively bright. Next, the various Luyten (Minnesota) series names are used (L, LB, LP). His published charts (Luyten 1949) are useful, and include some GL stars but also some important still unobserved binaries. The important Pleiades member LB 1497 (Luyten and Herbig 1960) is included with a modulus of 5.55. Ascription of certain DA stars to membership in the Hyades cluster or group seems somewhat uncertain. I use the list of van Altena (1969), a modulus of 3.20, and the designations (HG) from Giclas, Burnham, and Thomas (1962), which contains charts. In this utilitarian process I apologize that some famous names have unfortunately disappeared, GL 166B is 40 Eri B; HG7-255 is HZ 9; the first known magnetic white dwarf, +70°8247, is G260-15, but is also LFT 1446 and EG 129; the important cool DA with very large proper motion, LP9-231, appears as G259-21. For stars for which no chart has been published, I will provide them on request.

Preferentially, the parallaxes are from the U. S. Naval Observatory series under the leadership of K. Aa. Strand (Riddle 1970; Routly 1972; Harrington *et al.* 1975), from the Yerkes series, called Y (van Altena 1971; van Altena *et al.* 1973a, 1973b, 1975). Finally,

individually published values, and those from the *Yale Catalogue* are used and called "old." The system of weights is arbitrary. In Table III, the symbol *Q* is 1 for a recent  $p \geq 0''.068$ , 2 for  $0''.067 \geq p \geq 0''.040$ , 3 for  $0''.039 \geq p \geq 0''.020$ , and 4 for  $0''.019 \geq p \geq 0''.010$ . If the parallax is "old" *Q* is increased by unity. If the absolute magnitude is from cluster membership, *Q*=5, and if from membership in a resolved proper motion pair, *Q*=6. A few have measured *p* too small to be useful and are listed with *Q*=7 to elicit observer's attention. It is particularly unfortunate that the double white dwarf G206-17/18 (EG 373, 330) has no parallax. The *Q* symbols were used to set weights in fitting by least squares, unit weight for *Q*=1, 2, 5, 6 and half-weight for *Q*=3, 4. The list is still too small, containing 67 useful stars of which 19 are given half-weight, to settle many important astrophysical questions concerning degenerate stars, especially the width of the color-luminosity relation. The  $M_V$  for stars of *Q*=6 are obtained from calibration of the red companion by MC photometry of main-sequence stars of known parallax (Greenstein, in preparation). Their accuracy depends on the cosmic scatter in the color-luminosity relation for G-K-M stars.

#### II. THE COLOR-ABSOLUTE MAGNITUDE DIAGRAMS

The magnitudes observed for the parallax stars are given in Table II, and their colors listed in Table III together with the parallax  $M_{1.85}$ . The contents of Table II are described in the section labelled Data; *Q* in Table II is the quality of the MC scan; in Table III, *Q* is the quality of the parallax. In addition, in Table III the tangential motion in kilometers/sec, as derived from the parallax, is listed as *T*. The EG (or Gr) number is given, together with remarks, including suspected variability. Zeros are given for  $M_{1.85}$  when the measured parallax is too small to use (*Q*=7) and under *P* when a common proper motion modulus is used. The detection of EG 98 (HZ 43) as a source of soft x rays (Hearn *et al.* 1976; Margon *et al.* 1976a) and of extreme-ultraviolet radiation (Margon *et al.* 1976b) leads to its inclusion in Table III, in spite of its small parallax, given by Margon *et al.* (1976b) as  $0''.016 \pm 0''.004$ , from Allegheny measures and Lick observation of its dM companion. It helps define the upper hot end of the white dwarf sequence, together with EG 247 (G191B2B) a possible common proper motion star with a sdK companion. Both stars have half-weight. HZ 43B was noted as possibly variable by Eggen and Greenstein (1965), possibly observed during a flare; a 400 Å mm<sup>-1</sup> spectrum in 1971 showed it as of fairly early dM type with H $\beta$  and Ca II emission. The next brightest star, G238-44 (EG 102), has a poorly determined "old" parallax. It is unfortunate that the high-temperature end of the degenerate star sequence cannot be more accurately calibrated, even now.

The  $M_{1.85}$  is so close to the broad-band  $M_{V_c}$ , both centered on  $\lambda 5400$ , in a line-free region, that the table

## WHITE DWARFS

325

TABLE II. IDENTIFICATION, MAGNITUDES, MOTIONS OF DEGENERATE STARS

STAR	RA	DEC	MU	TH	LC	H	Q	P	I	R	V	G	B	U	R-I*	M <sub>1</sub>	M <sub>2</sub>	TYP <sub>E</sub>	E <sub>G</sub>	T	REF
CD408	0 2 28	72 50.4	3	25	-1	11.1	A	14.92	14.68	14.30	14.14	14.02	-0.3	1.5	DB	305	45				
G130-49	0 7 1	30 52.2	0.55	220	0	15.5	A	16.97	16.87	16.77	16.81	16.87	0.2	0.7	DC	1	136	6			
G21-37	0 9 39	50 9.0	0.75	210	0	13.8	B	14.30	14.35	14.46	14.59	14.79	-0.2	0.6	DA-F	381	44				
F11GE 4	0 17 24	13 36.0	0.04	77	8.1	A	15.90	15.68	15.27	15.07	14.94	0.2	1.5	DB	3	14					
G172-4	0 30 19	44 21.7	0.27	112	0	13.6	C	16.00	16.07	16.47	16.46	16.48	0.1	2.0	DA	300	72	b			
G158-100	0 31 22	-12 44.4	0.29	135	0	12.2	B	14.63	14.55	14.87	15.13	15.52	0.28	-0.4	DK-U	382	19				
G1-7	0 33 2	71 36.9	0.01	284	1.5	B	15.6	15.5	15.50	15.50	15.50	-0.4	1.5	DA	82						
G242-63	0 38 31	73 4.8	0.55	54	-1	14.8	B	16.38	16.43	16.14	16.04	16.01	-0.4	0.7	DB	383	163				
G270-48	0 41 15	-10 16.8	0.20	231	-1	11.0	B	15.19	15.06	14.48	14.46	14.37	-1.0	0.0	DC	267	39				
G1-27	0 46 30	35 10.0	2.97	154	1	14.7	A	12.30	12.31	12.41	12.50	12.80	-0.45	-0.4	DG	5	69	4,9			
G1-45	1 1 14	0 4 48.3	0.40	52	1	12.0	B	14.12	14.10	14.00	14.03	14.16	0.12	0.2	DA	7	27				
G269-160	1 23 2	-26 16.3	0.51	160	1.8	A	13.5	13.5	14.92	14.94	15.07	0.0	1.2	UC	307	45					
CD419	1 34 55	83 19.8	0.2	305	-1	8.9	A	13.61	13.55	13.06	12.83	12.68	0.1	0.1	DA	308	26				
G271-115	1 35 27	-0.5 14.8	0.66	122	0	11.9	A	12.78	12.83	12.91	13.05	13.40	0.1	0.6	UA	11	22				
PHL3802	1 46 24	-26 52.0	0.09	292	7.2	A	12.61	12.50	12.33	12.10	11.89	0.2	0.2	SDB	309	5	4				
CD421	1 47 22	67 24.6	0.2	100	-1	10.2	B	15.17	14.89	14.40	14.12	13.60	0.0	0.8	DA	310	60				
G71-41	1 51 38	0 1 46.7	0.36	95	0	12.7	A	15.40	15.46	14.88	14.73	15.37	0.1	2.3	DA	311	80				
G74-7	2 8 13	39 41.5	0.15	116	1.0	14.8	A	14.66	14.66	14.47	14.71	15.02	-0.04	-0.5	DA-F	166	82				
CD25	2 13 13	39 37.6	0.2	245	0	10.7	B	14.94	14.80	14.80	14.79	14.87	0.1	1.3	DA	312	17				
G134-22	2 13 47	42 44.5	1.07	127	0	16.4	B	15.85	15.97	16.30	16.53	16.91	0.37	-0.6	DC	16	108				
FEIGE 24	2 32 30	0 3 31.0	0.08	83	7.0	A	12.34	12.52	12.39	12.19	12.07	1.1.75	0.3	1.0	DAE	20					
G174-5	2 32 50	52 31.2	0.28	135	0	11.0	A	14.37	14.18	13.73	13.55	13.49	1.3.75	0.9	2.3	DA	314	48			
CD40	3 0 21	0 20.2	0.31	250	-1	9.9	B	16.05	15.85	15.36	15.30	15.30	0.2	1.2	DB	364	22				
G5-28	3 15 41	15 2.3	0.31	180	2	12.8	B	13.36	14.39	15.38	16.18	17.10	0.76	0.8	SMD	21	2,4				
G222-10	3 24 35	73 51.7	0.43	137	0	15.0	B	16.92	16.85	16.85	16.92	16.99	1.7.38	-0.3	0.8	DF-C	385	101	6		
G6-30	3 41 42	18 17.5	1.25	162	1	15.5	B	15.20	15.30	15.45	15.53	15.84	-0.09	-0.3	0.7	467U	24				
LRI47	3 49 6	24 47.0	0.06	144	10.6	B	17.30	17.06	16.57	16.35	16.03	0.0	1.2	DA	25	52	6				
H67-41	3 52 6	0 9 37.0	0.16	94	2	10.6	A	14.93	14.54	14.35	14.36	14.70	0.2	1.3	DA	26	34				
G7-17	3 58 42	18 36.1	0.24	166	2	16.0	B	13.97	14.65	15.47	16.20	18.35	1.0.06	1.7	SDM	27					
H68-7	4 1 30	25 1.0	0.25	149	10.9	A	14.25	13.91	13.77	13.77	14.16	0.0	3.2	DA	28	33					
HG7-112	4 6 18	16 59.0	0.12	101	10.6	A	10.6	10.2	15.63	15.26	15.10	15.37	-0.2	3.2	DA	29	32	6			
H22	4 10 6	11 45.0	0.11	150	9.2	A	14.48	14.03	13.79	13.71	13.76	0.1	2.2	DA	31	25					
GL166B	4 13 0	-0.7 44.0	4.08	33	12.5	A	11.05	9.87	9.50	9.30	9.29	9.52	0.0	2.2	DA	33	85	6,9			
H7-34B	4 26 50	58 53.3	0.31	146	-1	14.2	B	12.29	12.31	12.37	12.45	12.60	0.2	0.9	DAF-C	180	61	6			
HG7-255	4 29 24	17 38.0	0.11	108	9.0	A	12.58	13.55	13.88	13.97	14.04	14.33	-0.8	2.2	M+DA	36	35	6			
H2-7	4 31 0	12 35.0	0.09	89	9.2	A	14.73	14.23	14.02	13.91	14.01	0.5	2.6	DA	39	26					
GD61	4 35 10	41 3.7	0.2	165	10.8	B	15.52	15.58	14.90	14.68	14.62	14.55	0.3	1.4	DB	315	45				
LP475242	4 37 36	13 53.0	0.10	111	9.8	A	15.40	15.23	14.83	14.71	14.63	14.53	0.4	1.1	DB	316	23	6			
H2-14	4 38 12	41 28.2	1.1	285	0	8.6	A	14.05	13.86	13.60	13.48	13.35	0.2	1.6	DA	342	25	6			
G175-46	4 40 5	51 0.8	0.51	85	0	14.5	B	16.10	16.05	15.95	15.96	16.31	0.0	1.2	DA	317	93				
G191-16	4 55 21	55 20.8	0.30	227	0	13.4	B	16.45	16.27	15.98	15.83	16.28	0.3	2.7	DA	318	100				
G191-B28	5 1 30	52 46.0	0.10	160	6.7	A	12.54	12.30	11.75	11.67	11.66	11.27	0.3	0.8	DAM	247	13	6			
G069	5 32 48	41 28.2	1	285	9.0	A	14.67	14.67	14.64	14.64	14.63	15.15	0.0	1.0	DA	319	6				
G98-18	5 33 56	32 13.5	0.44	141	0	15.0	B	17.27	17.12	16.83	16.69	16.67	17.10	-0.3	2.1	DA	340	211			
GD290	5 43 35	57 58.3	2	120	11.5	B	15.95	15.81	15.63	15.60	15.75	16.04	-0.3	1.3	DA	341	26				

TABLE II (*continued*)

STAR	RA	DEC	MU	TH	LC	H	Q	P	I	R	V	G	B	U	R-I*	M1	M2	TYPE	E6	T	REF
699-37	5 48 46	-00 11 02	0.27	21	11.7 A	14.37	14.37	14.48	14.67	15.06	15.23	01	03	DC2P	248	15					
699-44	5 52 40	-04 9.2	2.44	167	1 16.6 8 1	14.07	14.22	14.65	15.11	15.68	17.40	0.37	-0.8	UK	45	90					
699-47	5 53 47	05 22.0	1.02	206	1 14.0 A 1	13.74	13.88	14.03	14.69	15.41	15.41	0.26	-0.6	DCP	290	41					
LTT2437	5 59 24	-12 30.0	0.26	77	11.5 B	12.92	14.07	14.39	14.65	14.96	15.62	-0.4	0.6	RSL	320	11	3				
687-7	6 44 15	37 34.9	0.97	190	-1 12.0 A 1	12.71	12.99	12.00	11.75	11.66	11.72	-0.48	JU	22	DA	50	102				
6250-26	6 48 40	6.4	7.6	0.48	199	0 15.0 B	16.35	16.42	16.62	16.87	17.05	-0.5	0.5	UA-F	342	63					
G107-70	7 27 6	48 17.4	1.34	191	2 15.4 B 1	14.14	14.26	14.74	15.16	15.05	16.85	0.43	-0.6	DC	52	53					
6234-4	7 28 49	6.4	16.0	0.29	173	1 13.6 B	15.65	15.76	16.33	16.67	17.09	0.35	-0.8	DC-K	321	27	2,3				
L745-46A	7 38 0	-17 17.0	1.25	115	13.4 B	12.98	12.98	12.91	12.94	13.08	13.27	-0.12	0.1	DF	54	49					
G089	7 43 54	44 16.3	2	210	-1 11.5 D	16.22	15.89	15.62	15.55	15.70	15.85	-0.4	0.2	DA	343	35	1				
6193-74	7 49 37	52 37.4	0.27	195	0 12.8 C	15.59	15.56	15.66	15.65	15.65	15.80	-0.2	0.5	DC	344	35					
G193-18	7 51 55	57 50.2	0.49	165	-1 13.5 A	15.35	15.44	15.06	15.01	15.03	15.05	0.02	0.0	UC	322	75					
G90-28	7 52 9	36 30.1	0.51	194	0 14.6 C 1	16.13	16.09	16.08	16.11	16.24	16.61	0.02	0.7	UA-C	345	65					
G111-54	8 2 18	38 41.0	0.31	187	-1 13.0 B 1	16.83	16.58	15.50	15.50	15.50	15.54	0.02	0.2	UF	346	72					
G0295	8 10 44	23 20.7	2	125	-1 11.0 C	16.66	16.48	16.01	15.85	15.96	16.16	0.08	0.2	DA	347	60					
G190	8 16 31	37 40.0	1	210	0 0.7 A	16.48	16.30	15.60	15.71	15.91	16.11	-0.6	0.9	UAP	346	13					
LD5235B	8 42 18	-18 48.0	0.13	247	1 11.2 A	16.10	16.01	15.61	15.49	15.38	15.37	0.02	0.6	DB	63	43					
G096	8 +6 2	34 40.9	0.2	280	-1 11.6 B	15.70	15.67	15.70	15.73	15.89	16.14	0.02	0.8	DA	323	21					
G117-18	8 56 11	33 8.7	0.34	271	0 12.8 A	15.39	15.25	15.14	15.22	15.03	15.07	-0.04	0.4	67U	182	45					
G252-27	9 0 25	73 27.0	0.60	210	1 15.9 C	16.46	16.36	16.36	16.98	17.32	17.76	0.24	-0.4	DC	349	69	2				
G195-19	9 12 27	53 38.6	1.56	222	0 14.8 A 1	13.94	13.94	13.84	13.94	14.22	14.41	-0.15	-0.3	UDXP	250	63					
G117B15A	9 21 13	35 29.8	0.14	264	-1 11.1 C 3	15.00	15.00	15.35	15.25	15.25	15.54	0.02	0.3	VDA	65	35	6				
G117-25	9 30 46	29 24.8	0.28	230	13.1 B 4	16.03	15.97	15.89	15.94	16.02	16.28	-0.02	0.5	DA	324	45					
G116-52	9 43 30	44 31.0	0.6	311	359 0	10.7 A 1	13.81	13.63	13.30	12.93	13.45	-0.50	0.0	39	DA	307	42				
G0303	10 11 17	57 3.5	0.16	139	-1 10.6 C	15.11	14.91	14.57	14.35	14.26	14.18	0.02	0.8	UB	386	40					
G235-67	10 19 38	63 42.7	0.39	48	0 12.6 B	14.59	14.59	14.66	14.70	14.92	15.29	0.02	0.6	DA	350	28					
G244-32	10 39 14	1.4	31.6	0.31	149	0 14.3 B	16.73	16.73	16.86	16.90	17.08	17.35	-0.1	0.8	VDA	72	61				
G0124	10 46 0	-01 45.3	2	195	0 11.7 C	16.26	16.00	15.78	15.84	15.25	15.54	0.2	1.4	DB	387	49					
G119-47	10 56 40	34 31.0	0.33	217	0 13.5 C	16.36	16.19	15.93	15.84	15.79	15.80	0.0	0.6	DC	325	96	1				
L970-30	11 5 30	-04 53.0	0.43	270	11.1 A	13.55	13.34	12.91	12.75	12.74	13.06	0.0	2.1	DA	76	46					
GC128	11 7 18	26 35.2	0.19	140	0 12.3 A	16.23	16.20	15.89	15.78	15.62	15.71	-0.5	0.6	DB	77	60					
G0305	11 8 12	56 21.0	0.22	149	0 13.6 A	17.40	17.05	16.86	16.90	16.99	17.38	0.02	0.8	VDA	351	61					
G120-45	11 21 38	21 38.1	1.07	272	0 14.3 A 1	14.17	14.10	14.12	14.22	14.35	14.63	-0.1	0.6	DF	79	63					
G0307	11 22 30	54 36.1	2	240	-1 11.2 C	15.96	15.71	15.35	15.1	15.20	15.54	0.4	2.2	DA	352	44					
G0310	11 26 30	38 25.4	1	255	-1 9.3 C	15.62	15.38	14.92	14.67	14.61	14.52	0.2	0.8	DA	80	25					
G147-65	11 33 5	35 50.9	0.51	261	1 14.2 B	13.59	14.82	15.63	16.37	17.01	17.59	0.02	0.8	M+DC	388	51					
G237-28	11 43 3	63 22.8	0.42	201	0 14.5 C	15.94	16.04	16.38	16.64	16.99	17.48	-0.2	0.4	DC-G	353	42					
G0312	11 49 6	41 3.8	2	300	-1 11.9 C	16.60	16.41	16.06	15.80	15.93	16.22	0.3	2.5	DA	354	58					
G255-2	11 59 12	80 21.7	0.28	263	-1 13.3 C	16.40	16.20	16.04	15.90	16.05	16.44	0.3	2.2	DA	355	78					
H-21	12 11 24	33 12.0	0.11	310	9.8 A	15.36	15.12	14.58	14.32	14.08	14.76	0.0	0.2	DO	86	51					
G0140	12 14 42	69 5.5	0.21	271	-1 15.6 B	17.00	16.94	17.08	17.26	17.48	17.93	-0.2	0.4	DC	356	97					
H-29	12 32 24	37 55.0	0.04	53	7.4 A	14.77	14.67	14.01	13.92	13.75	13.69	0.1	1.6	UB	351	91	7				
G61-17	12 44 45	14 58.8	0.44	300	0 14.0 C	16.15	16.05	15.83	15.15	15.86	16.21	0.1	2.0	DA	92	66	6				
Gn320	12 53 11	48 13.5	1	250	-1 10.8 C	17.03	16.84	16.46	16.35	16.35	16.71	0.4	2.9	DA	357	32					

## WHITE DWARFS

327

TABLE II (*continued*)

STAR	RA	DEC	MU	TH	LC	H	Q	P	I	R	V	G	B	U	R-I*	M1	M2	TYPE	EG	T	REF
G60-54	12 57 37	03 45-3	1.00	208	0	15-9 A	1	15-44	15-57	15-89	16-20	16-46	17-25	0-25	-06	0	DC	95	84		
G61-29	13 3 16	18 17-0	0.35	280	-1	13-7	8	16-14	16-08	15-89	15-65	15-65	16-45	0-25	-06	0	DBE	389	84	7	
H2-43	13 14 0	29 22-0	0.17	244	1	9-1 A	1	15-68	13-50	12-98	12-53	12-22	0-60	0-3	0-7	DWK	358	82	5		
G199-71	13 25 49	58 10-4	0.50	297	0	15-2 C	1	16-60	16-55	16-71	16-85	17-02	17-40	-04	14	DF	358	85			
G14-58	13 27 43	-08 18-8	1.30	249	1	12-8 A	1	12-71	12-51	12-20	12-11	12-08	12-40	-0-58	-0-2	29	DA	99	73		
G165-7	13 28 42	30 45-3	0.58	263	0	14-7 A	1	16-02	15-95	16-04	15-98	17-25	18-59	48	89	0	DC	391	89	2	
G0325	13 33 59	48 44-0	0.2	265	0	9-8 B	1	13-50	13-96	13-97	13-94	13-94	13-94	0-2	0	0	H+DB	359	15	7	
G64-43	14 34 10	03 56-7	3-87	254	1	17-6 C	1	13-96	14-14	14-68	15-12	15-60	16-84	0-0	0	0	DA	100	139	1	
G238-44	13 37 37	70 32-4	0.39	266	-1	10-7 A	1	13-45	13-22	12-76	12-52	12-46	12-53	0-6	26	DA	102	47			
*5843662	13 40 36	57 15-0	0.30	317	10-7 A	1	13-96	13-74	13-34	13-17	13-12	13-55	30	DA	103	35					
G63-54	13 44 59	10 36-0	0.87	265	0	14-8 B	1	15-09	15-09	15-06	15-17	15-33	15-66	39	96	0	DWK	360	82		
E0330	14 1 55	52 21-1	3	250	-1	13-3 C	1	16-39	16-39	16-40	16-45	16-55	16-79	00	13	0	DC	392	44		
G166-14	14 13 26	70 32-4	0.39	266	-1	10-7 A	1	16-26	16-09	15-90	15-71	15-76	15-69	04	18	0	DB	272	87		
G0335	14 19 57	35 8-6	1	150	-1	11-3 C	1	17-05	16-87	16-41	16-24	16-15	16-17	04	08	0	DA	326	162		
G223-63	14 26 12	61 23-7	0.32	269	0	14-5 C	1	16-91	16-91	17-00	17-17	17-30	17-65	08	10	0	UF-C	362	60		
E0337	14 33 6	53 48-5	1	295	-1	10-5 C	1	16-08	16-04	16-11	15-80	15-85	15-86	04	16	0	K+DA	363	38		
G66-32	14 48 24	07 46-1	0.92	241	-1	15-4 C	1	16-02	15-86	15-58	15-38	15-54	15-88	03	22	0	DA	111	243		
G0173	14 51 17	52 10-6	0.27	283	0	260	-1	11-1 A	1	15-85	15-61	15-20	14-81	02	36	0	DA	297	64		
G226-18	14 59 40	82 8-6	0.33	297	-1	12-4 B	1	15-31	15-15	14-78	14-64	14-25	14-49	00	12	0	DB	393	72		
G0340	15 8 44	63 43-8	1	210	0	9-1 C	1	15-09	14-97	14-71	14-63	14-79	15-10	03	19	0	DA	364	12		
C201-39	15 10 34	56 36-2	0.36	219	-1	14-0 C	1	16-55	16-44	16-26	16-26	16-33	16-03	00	19	0	DA	112	83	6	
E0185	15 31 30	-02 17-2	2	200	-1	9-8 A	1	14-51	14-33	13-90	13-73	13-70	13-83	04	22	0	DA	185	27		
G0347	15 34 48	50 23-7	2	150	0	11-7 C	1	15-90	15-87	15-81	15-80	15-89	16-19	00	14	0	DA	305	26		
G0190	15 42 4	18 16-1	1	165	-1	9-0 A	1	15-36	15-05	14-63	14-43	14-29	14-26	03	15	0	DB	193	23		
G0352	15 50 25	62 36-2	2	350	-1	12-7 C	1	16-92	16-85	16-78	16-78	16-89	17-00	07	14	0	UC	366	40		
G180-23	15 59 33	36 57-2	0.56	169	0	13-0 B	1	16-77	14-62	14-33	14-24	14-25	14-71	02	16	0	VDA	115	74		
G138-31	16 25 30	09 19-2	0.53	193	0	14-8 A	1	16-08	16-08	16-16	16-29	16-48	16-89	-07	13	0	UC	327	73		
G180-57	16 26 39	36 52-4	0.86	322	0	13-5 A	1	14-05	13-94	13-79	13-79	13-83	13-97	-027	01	26	DF	119	69		
G225-68	16 53 28	57 15-6	1	62	317	1	16-1 B	1	14-76	14-80	15-00	15-15	15-35	15-86	03	22	0	DC-F	258	115	6
G138-49	16 36 28	05 46-7	0.59	215	1	15-3 B	1	16-54	16-55	16-46	16-48	16-57	16-87	07	14	0	DAS	328	128		
G138-56	16 39 20	15 18-6	0.66	179	0	14-8 A	1	16-77	14-62	14-62	14-62	14-78	15-01	-02	16	0	DA	196	92		
G13356	16 39 49	53 46-9	3	225	0	11-9 A	1	15-23	15-07	15-05	15-10	15-23	15-21	-02	06	0	DC	329	24		
G225-38	16 41 16	73 16-0	0.32	340	0	14-0 B	1	16-74	16-68	16-50	16-51	16-52	16-71	03	19	0	UL-F	367	85		
G226-29	16 47 38	59 8-7	0.33	153	0	9-8 B	1	12-70	12-48	12-17	12-05	12-04	12-43	03	32	0	DA	368	20		
G169-34	16 55 1	21 31-7	0.56	176	0	12-8 A	1	14-31	14-18	14-06	14-10	14-44	-0-27	06	17	0	V2DA	197	48		
G181B58	17 6 58	33 16-8	0.14	170	2	11-6 D	1	16-31	16-17	15-83	15-67	15-72	16-15	-01	11	0	DA	198	44	1,6	
G240-47	17 10 8	68 23-4	0.27	349	0	14-6 B	1	17-35	17-35	17-49	17-59	17-75	18-21	-06	14	0	DF	365	68	2	
G240-51	17 13 28	69 34-9	0.36	191	-1	11-0 C	1	13-85	13-65	13-27	13-04	13-09	13-39	02	27	0	DA	370	42		
G140-2	17 36 14	05 17-9	0.28	187	0	13-0 B	1	15-97	15-89	15-80	15-82	15-88	16-20	-01	11	0	DA	371	48		
G240-72	17 48 53	70 52-7	1-68	312	1	15-4 A	1	13-54	13-69	14-21	14-34	14-49	15-07	-02	-03	0	UXP	372	74		
G229-21	17 56 24	82 45-2	3-63	337	0	17-0 C	1	14-25	14-25	14-35	14-35	14-47	14-81	08	19	0	DA	199	229	9	
G206-17	18 11 41	32 47-7	0.27	220	-1	13-5 B	1	16-40	16-35	16-39	16-45	16-54	16-84	00	11	0	U4-F	373	46	6	
G206-18	18 11 45	37 47-9	0.27	220	1	14-2 B	1	16-83	16-94	17-07	17-18	17-41	17-82	00	15	0	DC-F	330	50	6	
G227-35	18 29 21	54 45-2	0.36	318	1	13-4 B	1	15-45	15-42	15-53	15-75	15-87	16-33	-09	07	0	UXP	374	33		

TABLE II (*continued*)

STAR	RA	DEC	MU	TH	LC	H	Q	P	I	R	V	G	B	U	K-I*	M1	M2	TYPE	E_G	T	REF
G141-54	18 57 29	11 54 3	0.27	42	-1	12.7	B		15.86	15.75	15.55	15.44	15.50	15.92		00	2.1	DA	128	57	
G260-15	19 0 40	70 35 2	0.54	110	11.8	A	1	13.52	13.45	13.10	13.04	13.01	15.49		01	0.7	DXP	129	41		
G125-3	19 17 15	38 38 0	0.28	179	0	11.9	C	14.50	14.53	14.64	14.50	14.49	15.40		-04	0.9	DC	175	16		
G1754+1A	19 17 54	-07 45 0	0.19	205	8.6	A	1	12.61	12.66	12.24	12.17	12.16	12.36	-0.35	-02	0.6	DANK	131	9	o	
EC333	19 18 57	72 31 8	2	90	-1	11.0	A	15.81	15.52	15.12	14.82	14.70	14.82		03	2.5	DA	331	71		
L1573-31	19 40 24	37 24 0	0.20	174	11.0	A		15.15	14.92	14.52	14.41	14.25	14.21		-02	1.2	DB	133	43		
GD85	19 50 22	25 1.5	2	360	-1	11.0	C	15.54	15.39	15.13	14.98	15.14	15.49				DA	394	29		
GD387	20 3 59	43 45 7	2	45	-1	12.3	C	16.83	16.64	16.23	16.25	16.49				DA	395	64			
KZ SGE	20 5 19	17 33 4	0.08	170	9.8	A	15.62	15.53	15.32	15.19	15.26	15.20		00	2.0	VUAE	136	17	7,9		
G220-30	20 8 14	51 3.3	0.27	204	-1	13.4	B	16.84	16.65	16.21	16.05	15.97	16.46		01	3.4	DA	376	138		
G186-31	20 32 13	24 53.8	0.67	216	0	10.7	A	12.17	11.90	11.47	11.25	11.16	11.22	-0.63			DA	139	49		
GD543	20 9 58	62 16 7	2	195	-1	11.0	A	15.47	12.60	15.15	14.91	14.82	14.73		03	1.4	DA	332	48	5	
GD229	20 10 23	31 4.6	1	20	0	9.0	A	15.48	15.19	14.78	14.45	14.89	14.20		09	-1.9	DXP	333	19		
GD390	20 25 52	48 48 1	2	55	-1	11.7	C	16.20	16.06	15.85	15.75	15.91	16.25				DA	396	34		
ED391	20 28 5	3.4	2	60	-1	9.2	A	14.01	13.84	13.34	13.06	12.98	12.96		02	2.2	DA	397	32		
G212B1A	21 7 59	42 44.8	0.20	100	-1	12.4	B	16.31	16.21	15.90	15.81	15.80	15.79		01	1.0	DC	334	57	6	
GD1812B	20 54 6	-0.5	2.0	8.6	106	16.4	B	15.80	16.10	16.70	17.30	17.94	19.30		-10	1.0	DC	202	63	6	
GD392	20 58 20	34 14 5	2	45	-1	11.6	B	16.05	15.88	15.71	15.62	15.64	15.64		00	1.2	DC	396	37		
G187-15	20 59 41	31 37 0	0.50	213	-1	13.5	A	15.35	15.22	15.04	15.00	14.99	15.10		05	0.7	DC	262	76		
G144-51	20 59 46	1.9	1.2	0.31	200	0	13.8	B	16.22	16.26	16.37	16.48	16.63	17.03		-03	1.1	DANK	377	46	
G212B1A	21 26 43	73 25.8	0.34	169	0	10.4	A	13.29	13.12	12.68	12.52	12.48	12.82		03	3.0	DA	334	57	6	
GD394	21 11 3	4.9 53.7	2	89	-1	8.9	A	13.70	13.57	13.06	12.81	12.66	12.38		-03	0.8	DDP	399	26		
GD347	21 16 30	67 32.2	2	50	333	0	9.4	12.89	12.69	12.26	12.07	12.01	12.42		-01	2.8	DA	400	68		
G221-40	21 17 22	53 59.9	0.27	300	0	12.0	B	16.80	16.55	16.14	15.97	15.97	16.49		-04	3.5	DA	378	23		
G223-43	21 24 50	55 0.4	0.34	56	-1	12.3	A	15.15	15.00	14.63	14.48	14.45	14.85		00	2.9	DA	143	69		
G261-43	21 26 43	73 25.8	0.34	169	0	10.4	A	13.29	13.12	12.68	12.52	12.48	12.82		03	3.0	DA	144	35		
G226-10	21 29 41	-0.0	1.8	0.39	84	1	12.6	A	13.70	13.57	13.06	12.81	12.66	12.38		-03	0.8	DDP	399	26	
G226-27	21 40 22	20 46.6	0.71	200	0	12.2	A	13.43	13.35	13.22	13.25	13.30	13.43	-0.30	02	0.7	DC	396	37		
G226-31	21 44 58	-0.7	58.1	0.30	121	0	12.2	A	15.33	15.18	14.81	14.64	14.54	14.48		01	1.2	DB	149	75	
GD397	21 49 56	37 12.1	2	35	0	11.1	B	15.77	15.60	15.25	15.11	15.15	15.65		03	3.2	DA	401	36		
GD398	21 50 19	33 53.6	1	85	-1	9.6	B	15.87	15.61	15.17	14.97	14.88	15.16		03	2.3	DA	402	28		
G168-34	22 7 21	14 14 9	0.43	44	0	13.8	B	15.60	15.63	15.67	15.65	15.77	16.12		04	1.5	DA-F	302	60		
G223-19	22 34 36	52 47.6	2	226	-1	11.7	B	17.04	17.01	16.90	16.83	16.78	16.85		-02	0.9	DC	379	135		
G226-23	22 40 31	-0.1	43.4	0.34	209	0	13.8	B	16.40	16.31	16.15	16.15	16.24	16.55		00	1.7	DA-F	154	73	
GD399	22 46 39	22 20.5	0.52	83	0	12.9	B	16.70	14.56	14.33	14.26	14.32	14.60		-01	2.0	DA	155	61		
G128-7	22 48 57	29 23.7	1.26	82	0	16.1	B	15.18	15.25	15.54	15.78	16.05	16.79		-06	1.2	DA-F	283	100		
G156-64	22 53 12	-0.8	6.1	0.59	91	0	15.3	B	16.32	16.32	16.47	16.57	16.73	17.17		-05	0.7	DA-F	178	93	
GD404	23 2 25	45 43.2	2	75	-1	11.7	B	16.50	16.28	15.86	15.61	15.52	15.65		01	2.0	DA	403	80		
GD556	23 11 50	55 12.1	2	200	-1	12.1	B	16.62	16.47	16.21	16.09	16.07	16.63		00	3.0	DA	404	52		
GD559	23 19 15	69 9.9	1	260	-1	9.0	B	15.36	15.15	14.66	14.44	14.35	14.57		03	2.3	DA	303	24		
G128-62	23 23 28	25 36.0	0.29	154	1	14.3	D	16.65	16.75	17.02	17.21	17.53	18.07		-02	0.3	DANK	380	44	1	
GD248	23 23 36	15 43.8	1	210	-1	9.5	A	15.41	15.30	15.09	15.02	15.06	15.07		00	0.7	DC	335	13		
G29-38	23 26 16	04 58.5	0.56	237	0	11.7	A	13.46	13.29	12.98	12.85	13.36	-0.53		00	2.5	V2DA	159	49		
PG233712	23 37 42	12 21.3	1.2	49.6	1	13.3	A	13.39	13.30	13.08	12.98	12.96	13.16		04	0.6	VDA	336			
G130-5	23 41 21	32 16.2	0.27	254	0	10.0	A	13.42	13.23	12.89	12.77	12.76	13.20	-0.54	01	3.4	DA	162	23		
GD561	23 42 57	+80 40.2	0	15.37	15.1	1	A	15.37	15.04	14.54	14.28	14.05	13.78		02	1.0	DANK	304	405		
G30-20	23 47 20	12 49.5	0.36	78	-1	13.9	B	16.47	16.35	16.09	15.97	16.00	16.52		00	2.8	DA	405	111	6	

## Notes to Table II

The REF code is as follows: 1 is poor MC data; 2, poor  $U$  measure; 3, possibly neither main-sequence or degenerate; 5, member of resolved double; 6, member of common proper motion pair or cluster; 7, suspected spectroscopic or unresolved binary; 9, broad-band  $R \rightarrow I$  or radial velocity available. Under MU will be found the symbols 1, 2, 3, which refer to Lowell proper motion classes for the small-motion GD stars (Giclas, Burnham, and Thomas, Lowell Obs. Bulletin, Nos. 125, 141, 153). From estimates of the mean motion for these we adopt  $\langle 5 \log \mu_1 \rangle = -5.62$ ,  $\langle 5 \log \mu_2 \rangle = -4.12$ , and  $\langle 5 \log \mu_3 \rangle = -3.14$ . These result in less certain values of  $H$ ,  $T$ ,  $U$ ,  $V$ ,  $W$  and produce extra dispersion in the space motions. GR 397 was previously called EG 243; GR 399 = EG 244; GR 400 = EG 300; GR 402 = EG 281.

and the figures can serve equally well as visual absolute magnitude diagrams. Diagrams generated at other wavelengths could approximate photographic or near-infrared luminosities. The  $R^* - I^*$  colors would be useful if either metal-rich or very cool degenerates are found. The  $M_{1.85}$  are plotted in Figs. 1-5 with symbols permitting identification of the spectral classification. No clear dependence on space motion,  $T$ , is noted. For four of the diagrams a cubic fit was obtained by least squares, using weights already described. (The differences between the weighted and unweighted polynomials seldom exceed 0.12 mag.) The coefficients of the polynomials are given in Table IV, together with the mean deviation  $\sigma$  of the observed  $M_{1.85}$  of the parallax stars from the polynomial. The cubic fit has no physical meaning, but the  $\sigma$  show that  $G-R$  and  $G-I$  are good luminosity indicators,  $B-V$  only slightly inferior in spite of its steep slope ( $C_1 = 5.2$ ), and  $U-V$  the poorest indicator used. The cause is clearly seen in Fig. 3, where the Balmer jump,  $U-B$ , differs greatly between hydrogen-rich (DA) stars and hydrogen poor (DB, DC). Thus, in fact, the choice of  $(U-V)_c$  in the early calibration of  $M_{V_c}$  by Eggen and Greenstein (1965) was unfortunate. Although  $G-I$  and  $G-R$  colors are both determined at frequencies greater than the Paschen limit, apparently the slope in that region does not vary greatly with the hydrogen-to-helium ratio. The usefulness of the present  $B-V$  ([2.35] - [1.85]) suggests that photometry with a suitable set of moderately broad filters could be useful in the blue to visual region, if the bands excluded  $H\gamma$  and nearby He I lines.

Another determination of the scatter of points about the polynomials is provided by computing  $M_V(\text{ptm})$  from the polynomials for all three colors,  $G-R$ ,  $G-I$ ,  $B-V$ , and forming the  $\bar{M}_V$ . Compare this with the trigonometric  $M_{1.85}$  by forming  $\Delta M_V = M_{1.85}(\text{trig}) - \bar{M}_V$ . For 34 stars with  $Q=1, 2$ ,  $\bar{\Delta M}_V = +0.10 \pm 0.08$  with  $\sigma = \pm 0.44$ ; for 29 stars of  $Q=3, 4, 5, 6$ ,  $\bar{\Delta M}_V = -0.08 \pm 0.13$  and  $\sigma = \pm 0.68$ . The dispersions are smaller than in Table IV because errors introduced by the various colors (or blanketing effects) are independent and should average out. That part of the deviation introduced by the parallax error remains unchanged. Comparison of the  $M_V(\text{ptm})$  computed from the three different colors shows them to be remarkably accordant, with a  $\bar{\sigma} = \pm 0.17$ . The first possibility is that the color-luminosity relation for degenerate stars has remarkably small spread, and that the observed deviations from the mean are still largely caused by parallax errors.

Another possible interpretation is that all three colors used are highly correlated, and displace the star in the three different color-magnitude diagrams by similar vectors. For example, a composition difference might affect them all in a similar fashion, e.g., change the average slope of  $m_v$  from  $I$  to  $B$ . We will see that parallax errors may still be significant, and that further improvement in accuracy is needed for many of these stars.

The internal errors of a good recent parallax are quoted between  $\pm 0.^{\circ}002$  and  $\pm 0.^{\circ}004$ ; let us assume that the true errors may be twice as large as the internal errors. Consider the stars for which recent, large parallaxes exist,  $Q=1$ ,  $p \geq 0.^{\circ}068$ . There are 34 with  $\bar{p} = 0.^{\circ}089$ ; a  $\pm 1-\sigma$  plausible range of  $\bar{p}$  is  $0.^{\circ}081$  to  $0.^{\circ}097$ , or  $\pm 0.20$  mag. If  $\pm 2-\sigma$  range in true error is taken, the spread approaches  $\pm 0.39$  mag. But for 19 stars with  $Q=2$ ,  $\bar{p} = 0.^{\circ}056$ , and a  $2-\sigma$  true error give  $\pm 0.64$  mag. Thus, without asserting that true parallax errors are always double those internal errors quoted, a good fraction of the stars in the  $Q=1, 2$  sample have  $M(\text{trig})$  errors of  $\pm 0.30$  mag, which combines with the colorimetric errors (and differential blanketing) to suggest that most white dwarfs of a given color lie in a narrow band of luminosity. The dispersion must be less than quoted in Table IV (i.e.,  $< \pm 0.60$ ), very probably is less than  $\pm 0.44$  (from  $\Delta M_V$ ) and might conceivably be as low as  $\pm 0.17$  (from the agreement of  $M_V$  from the three different colors). This provides a very strong argument for a small range of radii and therefore of masses.

Use of small parallaxes has well-known systematic effects on the luminosities derived; one arises from the increasing asymmetry of errors in  $M$  as  $\delta p/p$  becomes larger. More serious is the selection effect, which is harder to evaluate; random choice among data with a normal distribution is prevented by the use of a lower limit to the acceptable parallaxes. A systematic error which, it is hoped, is less than 0.30 mag might be expected at the bright end, where the parallaxes are all small. The statistical corrections vary as  $\sigma^2$ , and we may be considerably underestimating their importance. Probably, future discovery and calibration of very hot degenerates in common proper motion pairs will provide the needed calibration at the bright end.

Omitting the uncertain, hottest stars, EG 98, 247, all the degenerate stars of known parallax lie between  $9.9 \leq M_{1.85} < 15.7$ . The hot stars extend the bright limit to 8.4; it should be remembered that, at a fixed radius,  $M_{1.85}$  will increase only linearly with tempera-

TABLE III  
WHITE DWARFS OF KNOWN PARALLAX

STAR	P	Q	G-R	M1.85	G-I	R - I	R*-I*	U-B	B-V	U-V	T	TYPE	EG	REMARKS
1 G130-49	.0	6	-0.03	14.20	-0.06	-0.03		0.21	0.10	0.31	86	DC	1	CPM G130-50
2 G172-4	.0	6	-0.21	11.70	-0.20	0.01		0.37	0.01	0.38	77	DA	306	CPM G171-62 ??
3 G1-7	.026	3	-0.35	12.64	-0.46	-0.11		0.28	0.01	0.29	72	DA	4	
4 G1-27	.239	1	0.19	14.30	0.20	0.01	-0.05	0.65	0.39	1.04	56	DG	5	
5 G1-45	.045	2	-0.07	12.27	-0.09	-0.02		0.29	0.16	0.45	38	DA	7	
6 G271-115	.061	3	0.13	11.76				0.35	0.22	0.57	51	DA	11	OLD P TOO SMALL
7 G74-7	.064	2	0.14	13.50	0.13	-0.01	-0.04	0.31	0.24	0.55	85	DA-F	168	Y.042
8 G134-22	.037	3	0.56	14.08	0.68	0.12	0.37	0.93	0.61	1.54	133	DC	16	OLD P.049
9 G221-10	.026	3	0.07	13.92	0.0	-0.07		0.39	0.14	0.53	78	DF-C	385	
10 G6-30	.072	2	0.25	14.58			-0.09	0.31	0.23	0.54	73	4670	24	W219;P ONE SOURCE
11 LB1497	.0	5	-0.72	11.00	-0.96	-0.24		-0.20	-0.33	-0.53	40	DA	25	PLEIAU
12 HG7-41	.022	5	-0.58	11.20				0.34	-0.18	0.16	36	DA	26	HYAD
13 HG8-7	.036	3	-0.48	11.69				0.39	-0.14	0.25	34	DA	28	OLD P.051
14 HG7-112	.023	5	-0.53	12.06				0.29	-0.18	0.11	28	DA	29	HYAD
15 GL166B	.205	1	-0.57	11.07	-1.02	-0.45		0.23	-0.21	0.02	92	DA	33	40ERI;CPM
16 G175-34B	.179	1	0.14	13.63	0.16	0.02		0.26	0.23	0.49	63	DAF-C	180	CPM Y P.170
17 HG7-255	.023	5	0.42	10.68	1.39	0.97		0.29	0.16	0.45	28	M+DA	38	COMPOSITE HZ9
18 HZ-7	.023	5	-0.71	11.03				0.10	-0.32	-0.22	28	DA	39	
19 LP475242	.023	5	-0.51	11.64	-0.67	-0.16		-0.10	-0.21	-0.31	28	DB	316	POSSIBLE HYAD
20 HZ-14	.023	5	-0.80	10.66				-0.13	-0.38	-0.51	28	DA	42	HYAD
21 G191B2B	.021	3	-0.84	8.36	-1.08	-0.24		-0.32	-0.48	-0.80	22	DANK	247	CPM SDK
22 G98-18	.003	7	-0.37	0.0	-0.51	-0.14		0.31	-0.15	0.16	0	VDA	343	PARALLAX TOO SMALL
23 G99-44	.155	1	0.89	15.60	1.04	0.15	0.37	0.72	1.03	1.75	75	DK	45	OLD P.166
24 G99-47	.122	1	0.50	14.55	0.64	0.14	0.26	0.72	0.58	1.30	40	DCP	290	
25 G87-7	.058	2	-0.74	10.81	-0.96	-0.22	-0.48	0.06	-0.34	-0.28	83	DA	50	
26 G107-70	.098	1	0.90	14.70	1.02	0.12	0.43	1.20	0.91	2.11	66	DC	52	CPM Y P.092
27 L745-46A	.142	1	0.01	13.67	-0.04	-0.05	-0.12	0.19	0.17	0.36	41	DF	54	CPM
28 G90-28	.029	3	0.02	13.40	-0.02	-0.04		0.37	0.16	0.53	83	DA-C	345	
29 G111-54	.023	3	-0.33	12.38	-0.50	-0.17		0.04	-0.08	-0.04	63	DF	346	
30 G47-18	.047	2	-0.03	13.50	-0.17	-0.14		0.04	-0.11	-0.07	35	4670	182	
31 G195-19	.100	1	0.10	13.84	0.0	-0.10	-0.15	0.29	0.28	0.57	76	VDXP	250	VAR
32 G117B15A	.0	6	-0.45	11.33	-0.65	-0.20		0.40	-0.10	0.30	45	VDA	65	CPM; VAR
33 G117-25	.030	3	-0.03	13.28	-0.09	-0.06		0.26	0.13	0.39	44	DA	324	
34 G116-52	.028	3	-0.63	10.44	-0.81	-0.18	-0.50	0.52	-0.27	0.25	54	DA	67	
35 G120-45	.071	1	0.12	13.37	0.05	-0.07	0.16	0.28	0.23	0.51	72	DF	79	OLD P.J84
36 G61-17	.0	6	-0.30	12.61	-0.40	-0.10		0.35	0.03	0.38	93	DA	92	CPM
37 G60-54	.082	1	0.56	15.40	0.66	0.12	0.25	0.79	0.60	1.39	59	DC	95	
38 HZ-43	.016	4	-0.80	9.00	-0.98	-0.18	-0.60	-0.31	-0.45	-0.76	51	DANK	98	CPM; JNPUBL. P
39 G14-58	.067	2	-0.40	11.33	-0.60	-0.20	-0.58	0.32	-0.12	0.20	92	DA	99	CPM; OLD P.062, Y
40 G62-53	.117	1	0.98	15.02	1.16	0.18		1.24	0.92	2.16	158	DA	100	OLD P.135
41 G238-44	.027	4	-0.70	9.92	-0.92	-0.22		0.07	-0.30	-0.23	67	DA	102	
42 G63-54	.048	2	0.08	13.46				0.33	0.27	0.60	87	DANK	360	
43 G66-32	.003	7	-0.48	0.0	-0.64	-0.16		0.34	-0.04	0.30	0	DA	111	PARALLAX TOO SMALL
44 G201-39	.0	6	-0.18	11.67	-0.29	-0.11		0.30	0.07	0.37	83	DA	112	CPM
45 G180-23	.034	3	-0.40	11.97	-0.56	-0.16		0.45	-0.11	0.34	76	VDA	115	VAR
46 G180-57	.059	2	-0.15	12.65	-0.26	-0.11	-0.27	0.14	0.04	0.18	72	DF	119	Y P.063
47 G225-68	.068	1	0.37	14.15	0.41	0.04	0.10	0.52	0.34	0.86	115	DC-F	258	CPM Y P.074
48 G138-56	.006	7	0.04	0.0	0.05	0.01	-0.01	0.32	0.12	0.44	0	DA	196	PARALLAX TOO SMALL
49 G169-34	.042	2	-0.18	12.18	-0.31	-0.13	-0.27	0.34	0.04	0.38	67	DANK	197	SUSP. VAR.
50 G240-47	.0	6	0.24	14.94				0.46	0.26	0.72	40	DF	369	CPM
51 G140-2	.023	3	-0.07	12.61	-0.15	-0.08		0.32	0.08	0.40	59	DA	371	
52 G240-72	.164	1	0.67	15.31	0.83	0.16		0.58	0.31	0.89	49	DXP	372	
53 G259-21	.057	2	0.10	13.03				0.34	0.22	0.56	302	DA	199	Y P.063
54 G206-17	.0	6	0.10	0.0	0.05	-0.05		0.30	0.15	0.45	0	DA-F	373	CPM DOUBLE WD
55 G206-18	.0	6	0.27	0.0	0.35	0.08		0.41	0.24	0.65	0	DC-F	330	CPM DOUBLE WD
56 G260-15	.082	1	-0.41	12.67	-0.48	-0.07		-0.03	-0.06	-0.09	32	DXP	129	Y P.081
57 G125-3	.084	1	0.21	14.28	0.23	0.02		0.44	0.31	0.75	16	DC	375	
58 GL754.1A	.098	1	-0.29	12.19	-0.44	-0.15	-0.35	0.0	-0.12	-0.12	10	DA	131	CPM P.102 LDS6788
59 G186-31	.066	2	-0.65	10.57	-0.92	-0.27	-0.63	0.06	-0.31	-0.25	50	DA	139	P.069
60 GL812B	.064	2	1.20	15.73	1.50	0.30		1.39	1.21	2.60	64	DC	202	CPM P.J68
61 G187-15	.028	3	-0.22	12.31	-0.35	-0.13		0.11	-0.05	0.06	83	DC	262	
62 G144-51	.025	3	0.22	13.37	0.25	0.03		0.40	0.26	0.66	59	DANK	377	
63 G212B1A	.0	6	-0.40	11.77	-0.50	-0.10		-0.01	-0.10	-0.11	64	DC	334	CPM
64 G231-43	.029	3	-0.52	11.94	-0.67	-0.15		0.40	-0.18	0.22	56	DA	143	OLD P.058
65 G261-43	.045	2	-0.60	10.94	-0.77	-0.17		0.34	-0.20	0.14	33	DA	144	
66 G26-10	.021	3	-0.47	11.83	-0.60	-0.13	-0.52	-0.05	-0.19	-0.24	69	DB	145	Y.033; MEAN USED
67 G126-27	.074	1	-0.10	12.57	-0.18	-0.08	-0.30	0.13	0.08	0.21	46	DC	148	
68 G26-31	.011	4	-0.54	11.31	-0.69	-0.15	-0.06	-0.17	-0.23	72	DB	149	OLD P.052; WT MEAN	
69 G67-23	.050	2	-0.30	12.83	-0.44	-0.14		0.28	-0.01	0.27	50	DA	155	
70 G128-7	.049	2	0.53	13.99	0.60	0.07		0.74	0.51	1.25	123	DA-F	283	Y P.043
71 G29-38	.071	1	-0.43	12.24	-0.61	-0.18	-0.53	0.48	-0.10	0.38	39	DA	159	VAR?
72 G130-5	.056	2	-0.46	11.64	-0.65	-0.19	-0.54	0.44	-0.13	0.31	23	DA	162	CPM

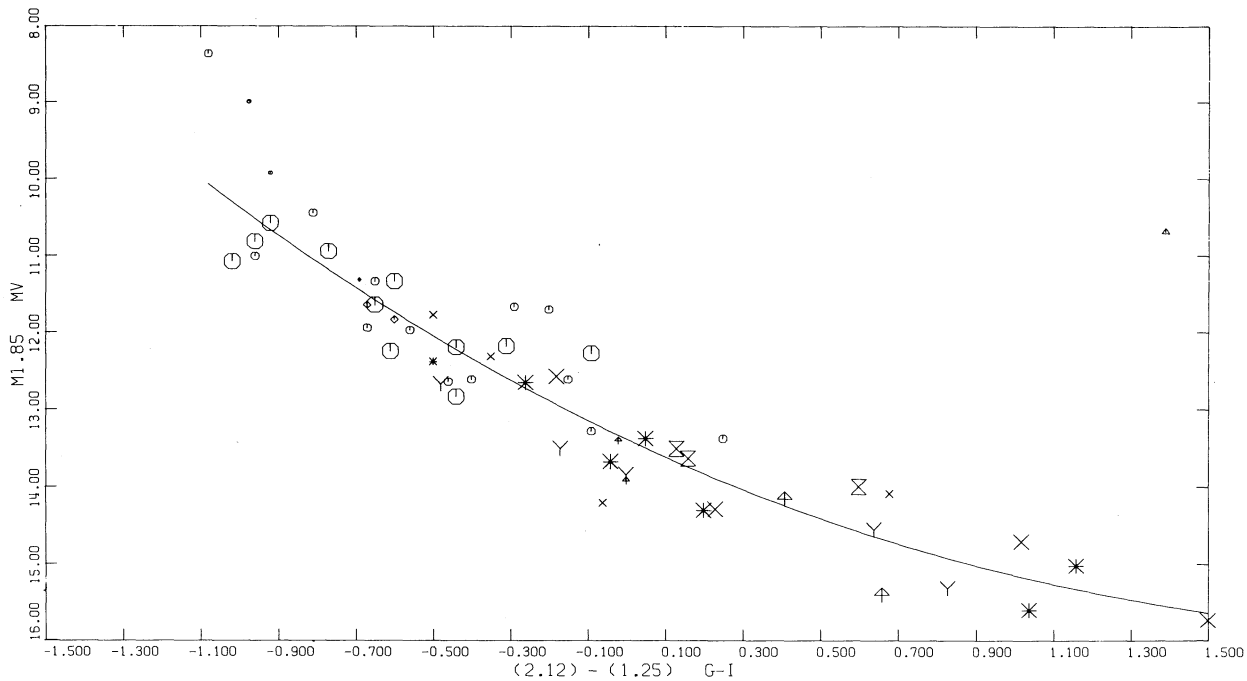


FIG. 1. The absolute magnitude  $M_{1.85}$  (or  $M_V$ ) of degenerate stars of known distance as a function of MC  $G-I$  color ( $1/\lambda=2.12$  to  $1/\lambda=1.25$ ). The third-degree polynomial plotted is fitted by least squares, with a mean error  $\sigma(M_V)=\pm 0.56$ . The size of the plotted point reflects the quality of parallax;  $Q=1, 2$  largest,  $Q=4$  smallest. Symbols for the spectral type in this and following figures are DB, diamond; DA, octagon; DC, X; DA,F  $\times$ ; borderline types DA-DC, or DF-DC, triangle with vertical bar; DF, DG, DK, star; composite, open triangle; polarized DP, Y; carbon ( $\lambda 470$ ), Z. The discrepant point at the upper right is EG 38 (HG7-255), a composite dMe+DA. The DA and DB stars are well mixed. Calibration in terms of effective temperature and radius is in Table VI.

ture. A blackbody of infinite temperature has  $G-I = -1.15$ ,  $G-R = -0.84$ ,  $B-V = -0.52$ , and very hot stars would therefore lie along a nearly vertical locus at those colors. Inspection of Table V shows few

extremely hot, bright stars; the predicted  $M_{1.85}$ , from their colors, for the bluest, are 9.8 for EG 310 (GD 421), 9.6 for EG 86 (HZ 21), and 9.7 for EG 304 (GD 561). The cooling times for the hottest degenerates

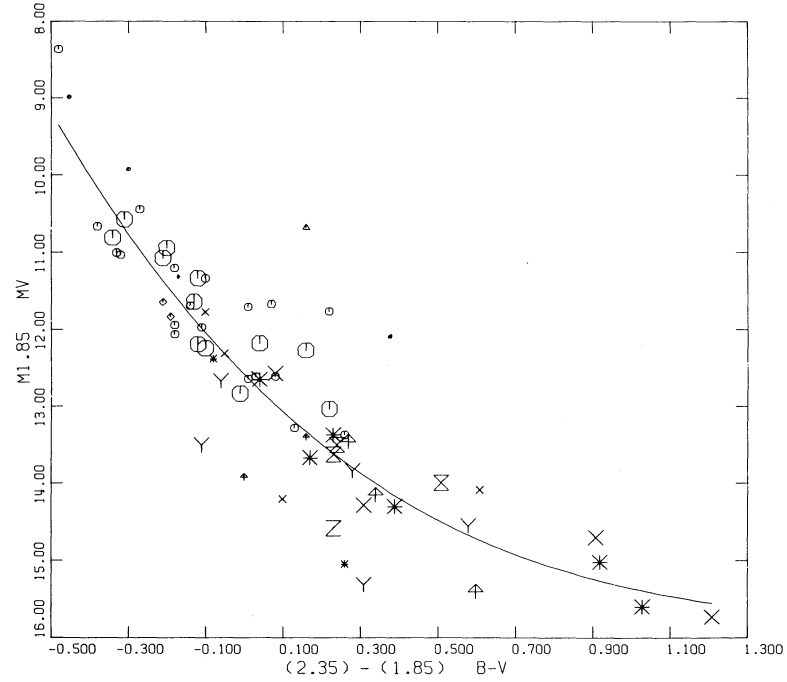


FIG. 2.  $M_{1.85}$  as a function of  $B-V$ ; the scatter is  $\pm 0.62$ , and is probably increased by the effect of Hy in DA stars. The DA stars are slightly displaced, systematically to the right, or above the DB. Somewhat larger deviations occur in DF or DC stars, possibly from line blocking.

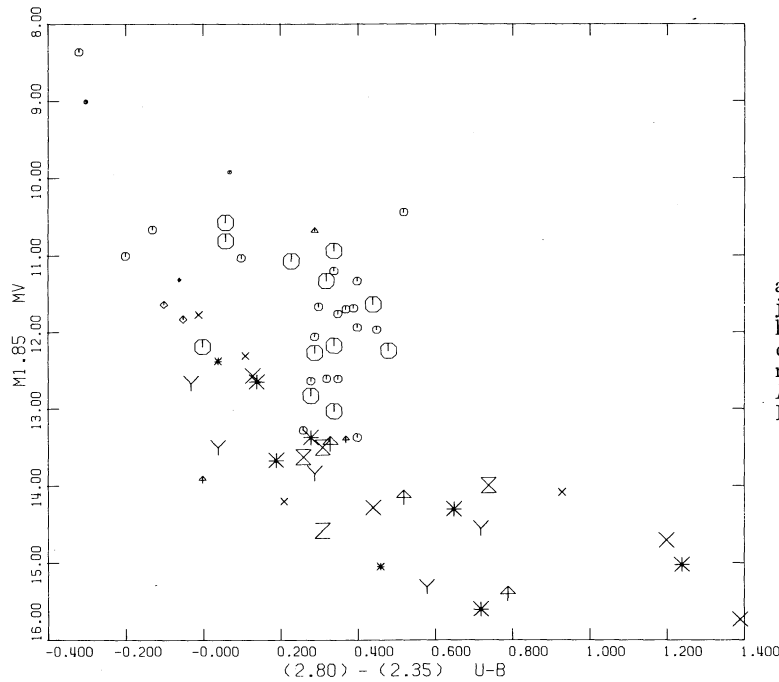


FIG. 3.  $M_{1.85}$  as a function of  $U-B$ . There is almost no relation for the DA stars. The Balmer jump dominates and in hydrogen-rich stars the locus of increasing temperature runs nearly vertically. The helium (DB) or the presumably helium-rich DF-DK show a nearly normal dependence of  $M_{1.85}$  on color, and are continuous with the hot DAs.

must be very short, since they are quite rare in space. Among the 178 stars in Table V not one has  $M_{1.85} > 15.7$ , the luminosity of the long known GL 812B, EG 202. Extremely cool, faint degenerates have therefore not been found in the MC survey of stars of large proper motion. Over 30 stars have been added with  $M_{1.85} > 13$ , and these will be worth measurement, both for parallax and circular polarization, which seems relatively common among the fainter stars. Fuller discussion of

the statistics of luminosities and temperatures of frequency in space will, it is hoped, appear in the near future. Figure 6, however, is the observed frequency distribution of  $M_{1.85}$ , derived from data on 178 degenerate stars in Table V. The median observed  $M_{1.85}$  is +12.2. The counted number per half-magnitude interval is shown as  $\psi(M)$ , uncorrected for selection effects in discovery, or for volume of space surveyed. Clearly, the sample begins to be incomplete at  $M > 11.5$ .

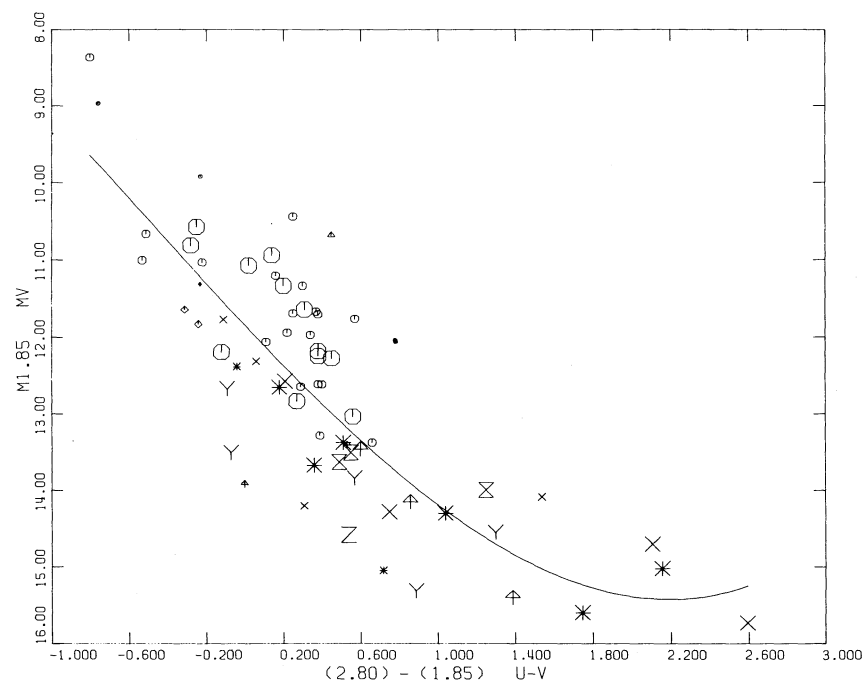


FIG. 4.  $M_{1.85}$  as a function of  $U-V$ , shows a better correlation than Fig. 3, but the separation of the hydrogen-rich DA stars persists.

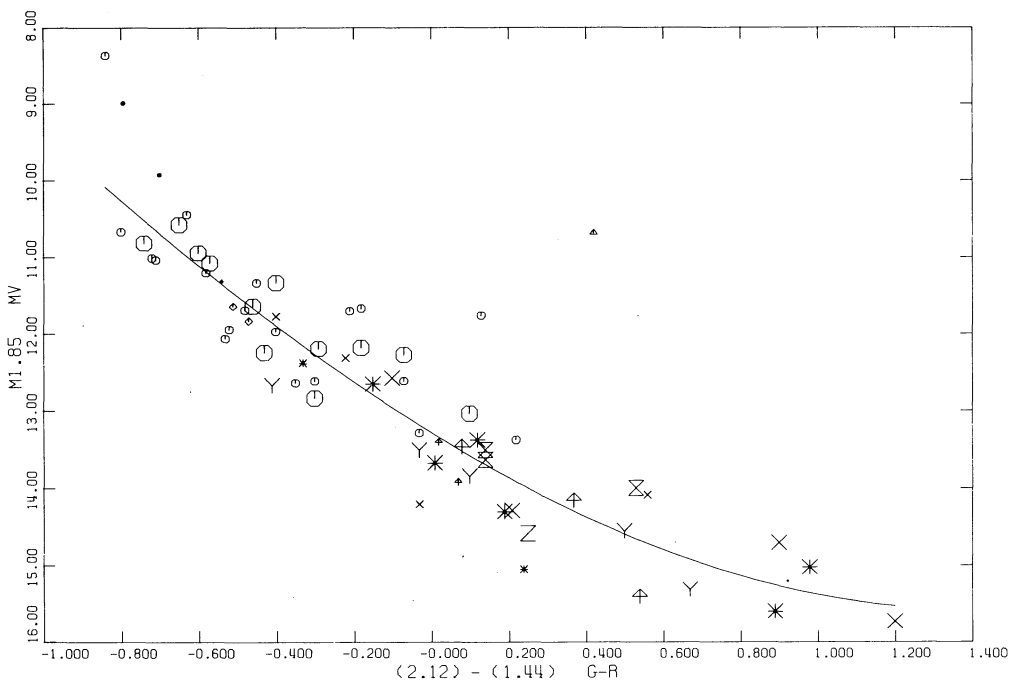


FIG. 5.  $M_{1.85}$  as a function of  $G-R$  is a generally most useful correlation, with  $\sigma = \pm 0.58$ . Model-atmosphere calibration of the fitted cubic in terms of temperature is not as good as for  $G-I$ , because of the relatively larger effect of errors in the fluxes computed from the models.

From cooling theory, the true luminosity function  $\phi(M)$  should increase roughly as  $L^{-5/7}$ . Between  $M=10$  and  $M=15$ ,  $\phi(M)$  should increase by  $10^{10/7}$ , or 27 times. The volume is reduced by 1000, so we should see 0.027 as many stars at +15 as at +10. The detection of any degenerate star at  $M=15$  shows how strongly selection has been favoring red degenerates, by search among the yellow or red proper motion stars.

### III. ASTROPHYSICAL IMPLICATIONS

The figures displaying the color-magnitude diagrams for the parallax stars show that the hydrogen-rich and helium-rich stars follow generally the same course except for differences obviously caused by the hydrogen spectrum itself. Only one star (open triangle) HG7-255 (EG 38) which is a composite DA+dMe is grossly displaced from figure to figure, dependent on which color is used. The polarized stars (symbol Y) are known to have distorted continua, yet lie near the mean curves in the  $G-I$  and  $G-R$  plots. The DA stars (octagons) are near the mean curves in  $G-I$  and  $G-R$ , are somewhat displaced (upwards or to the right) in  $B-V$ . It is impossible to find a useful locus in the  $M$ ,  $U-B$  and  $M$ ,  $U-V$  plots for the DAs. In fact, over a considerable range of temperature (6000–15 000°K) bracketing the maximum strength of the Balmer jump,  $U-B$  remains nearly independent of  $T$ , while the luminosity increases as  $T^4$ . If all stars had the same radii this would cause a displacement and scatter among the DA stars in the  $U-B$  and  $U-V$  plots, as observed. There is a small

displacement, depending on composition in the  $M$ ,  $B-V$  diagram. Cool stars with metallic lines (DF-DG-DK) may also be displaced from those with very weak lines (DC) by amounts which apparently increase towards the ultraviolet. Investigation of  $M$ ,  $R-I$  and  $M$ ,  $R^*-I^*$  fails to reveal any interesting displacements, but for these the color range is small and the available colors are too few.

Model-atmosphere analyses of narrow-band colors and scans of white dwarfs, study of their continua and line profiles, suggest that there is only a small range in  $\log g$ , for the DA and a few DB studied. The known masses cover a range of 2.5 so that the radius might decrease by this factor between a star like 40 Eri B and  $\alpha$  CMa B. At a fixed temperature, this range of radius produces two magnitudes total range in bolometric luminosity. We can now say that the typical range in luminosity (i.e., mass) from the parallax stars is less than this, from the spread in the Figs. 1, 2, and 5. Is there any systematic variation in radius with luminosity or color? Can we account numerically for the

TABLE IV. Coefficients of polynomial fits  $M_V$ , color.

$M_V$ from	$C_0$	$C_1$	$C_2$	$C_3$	$\sigma$	Figure
$G-I$	13.421	2.2011	-0.9037	0.3262	0.559	1
$G-R$	13.290	2.8195	-1.3313	0.5775	0.584	5
$B-V$	12.593	5.1894	-3.9600	1.4742	0.623	2
$U-V$	11.797	2.8823	-0.5187	-0.0251	0.830	4

TABLE V  
PREDICTED LUMINOSITY, PARALLAX, SPACE MOTION AND TYPE FOR DEGENERATE STARS

EG	MV or Gr	P ptm	P trig	U	V	W	Type	$\Delta M$	Note	Gr	WV ptm	P trig	U	V	W	Type	$\Delta M$	Note
305	11.22	24	34	-23	18	DB	... DC	-1.02		42	10.03	1.7	(23)	7	-13	20	DA	+0.63
1	13.18	19	-116	0	-75	DB	... DA-F	-3.3		317	13.04	2.6	19	-52	75	DA	...	
381	13.94	79	-28	6	-33	DB	... DA	+1.03		318	11.78	1.4	16	-2	-99	DA	...	
3	10.77	13	13	-5	0	DA	... DK-G	-40		247	11.56	3.6	21	-5	-1	-4	DA	-1.20
306	12.73	18	(11)	51	-40	DA	... DA	+0.32		319	13.43	5.7	(3)	-14	-209	23	DA	...
382	14.66	91	4	-14	-4	DA	... DA	-38		340	11.76	1.0	6	-21	1.3	DA	...	
4	12.32	22	26	-64	-38	DA	... DB	-86		341	12.77	2.7	3.3	-14	-209	11	DC	...
383	12.12	16	... (87)	106	-86	DA	... DA	-38		248	14.23	8.9	7	-22	12	DC2P	...	
267	11.43	25	... 199	239	-4	DA	... DC	-7		45	15.21	12.9	155	-48	-73	11	DK	+0.39
5	13.20	69	45	25	0	DA	... DA	+0.40		290	14.53	1.22	-14	-20	-33	DCP	+0.02	
307	13.58	53	-13	-43	1	DC	... DA	-1.84	2,6	320	14.62	11.1	1	-4	10	DG?	...	
11	13.60	143	61	8	-20	DA	... DA	-1		350	10.35	4.7	58	-17	-85	53	DA	+0.46
309	11.88	14	... (87)	14	2	4	... DA	-1		342	14.38	3.6	38	-11	-30	DA-F	...	
310	9.80	14	... 11.57	14	47	-38	3	DA	...	52	15.14	12.0	98	18	-46	-19	DC	-0.44
311	11.57	68	64	50	-64	DA	... DA	-10		321	14.86	5.1	12	-24	1	DC-K	...	
168	13.62	68	26	50	-64	DA	... DA-F	-0.12		54	13.33	1.22	-33	-23	28	DF	+0.34	
312	12.87	41	... 72	-11	7	DA	... DA	-11		343	12.21	2.1	13	-25	-21	DA	...	
116	14.61	46	37	60	-84	-31	DC	-0.53		344	13.44	3.6	14	-30	-11	DC	...	
26	10.52	(42)	... 28	13	... 28	DA	... DA	1,5		322	12.51	3.1	31	-68	-9	DC	...	
314	10.98	17	... 11.57	14	56	-55	16	DA	...	345	13.34	2.8	29	14	-76	36	DA-C	+0.06
384	11.57	17	... 20	26	75	-64	DA	-10		346	12.14	2.1	23	9	-68	-21	DF	+0.24
21b	... 13.37	... 20	... 72	-8	-93	-43	DA-F-C	-0.55		347	11.40	(1.2)	...	-32	-41	31	DA	...
385	13.81	50	50	8	-93	-9	DA	-0.59		348	(12.58)	(24)	4	-10	-7	DAP	...	
24	13.81	50	72	-8	-93	-43	DA	-0.59		63	11.44	15	14	-6	-40	DB	...	
25	10.41	6	(8)	13	-24	DA	-0.14	-0.14		323	13.45	3.5	13	5	-16	DA	...	
26	11.34	23	(22)	13	-24	DA	-0.14	-0.14		182	(12.73)	(3.3)	47	30	3	34	DA	+0.77
27	10.24	27	... 36	3	-32	-8	DA	-0.00		349	14.92	3.9	50	-53	-6	DC	...	
308	11.69	36	17	(23)	10	-25	DA	+0.61		350	13.57	8.8	100	47	-61	-31	VEXP	+0.27
29	11.45	17	31	10	-25	17	DA	-0.59		250	13.57	8.8	100	47	-61	-31	VDA	...
31	10.57	20	20	-2	-25	-4	DA	-0.17		65	11.77	1.9	16	24	-30	-25	VDA	-0.44
32	11.54	23	20	56	22	DA	-0.17	-0.17		324	13.20	2.9	30	20	-30	-27	VDA	+0.08
33	11.24	223	205	-50	-10	DA	-0.03	-0.03		350	13.73	6.5	...	-21	-24	-5	DA	-0.48
180	13.66	181	179	33	-29	18	M+DA	1		325	11.64	1.5	...	-18	-21	3	DA	...
38	10.52	18	(23)	7	-16	19	DA	+0.51		325	11.97	1.6	46	40	-15	-18	DA	...
315	10.90	16	16	11	-39	-20	DB	-0.23		76	11.23	4.6	...	-50	-30	12	DB	...
316	11.41	21	(23)	3	-20	11	DB	-0.23		386	10.99	1.9	...	-21	-24	25	DB	...
351	12.92	71	56	-21	-36	DA	-0.17	-0.17		350	13.73	6.5	...	-18	-21	3	DA	...
352	11.42	16	16	28	-33	-4	DA	-0.20		72	13.67	2.3	...	-48	-38	1	VDA	...
80	10.49	13	13	19	-15	-7	DA	-0.00		366	13.09	1.8	...	-12	-39	-28	DC	...
388	10.45	41	41	13	-9	-4	DA	-0.14		387	11.97	3.5	34	-68	-28	-10	VDA	-0.07
184	10.45	45	45	5	-38	-4	DA	-0.14		327	13.86	3.5	-39	-60	-14	-18	DC	...
353	14.65	55	55	-21	-36	DA	-0.14	-0.14		367	12.77	1.8	-39	-60	-14	-18	DC	...
354	11.46	12	12	66	-41	-7	DA	-0.00		368	11.74	8.2	60	-2	34	DF	-0.14	
355	12.21	17	17	49	-10	-9	DO	-0.14		119	12.79	6.3	101	-32	44	-4	DC	+0.05
86	(9.63)	(10)	85	-45	-14	DC	-0.14	-0.14		258	14.10	6.6	...	-41	-121	12	DA	...
356	14.05	25	25	-3	8	-1	VDB	7		328	13.15	2.2	...	-64	-59	-30	DA	...
91	10.75	21	(23)	95	-5	9	DA	+0.14		198	11.75	15	...	-39	-15	-14	DA	...
92	12.47	21	21	...	...	...	...	...	...	...	...	...	...	...	...	...	...	

## WHITE DWARFS

335

TABLE V (CONT'D)

EG	MV or Gr.	P ptm	P trig	U	V	W	Type	ΔM	Note	EG or Gr.	MV or Gr.	P ptm	P trig	U	V	W	Type	ΔM	Note
357	11.66	15	•••	19	-25	4	DA	•••		369	13.83	19	(31)	67	-10	-1	DF	+1.11	
95	14.66	57	82	-4	-79	-28	DC	+0.74		370	11.17	38	•••	-40	-2	14	DA	•••	
389	(12.45)	(20)	•••	76	-35	3	DBE	•••	-0.89	371	13.04	28	23	-27	-16	DA	-0.43		
98	9.89	24	16	15	-28	3	DWK	•••		372	(14.44)	(111)	164	47	-36	44	DXP	+0.87	4
358	13.94	28	•••	82	-21	-9	DF	•••	-0.53	199	13.58	73	57	191	-117	47	DA	-0.55	
99	11.86	86	•••	42	-59	-5	DA	•••	-0.53	373	13.45	26	•••	-34	-27	15	DA-F	•••	
391	13.33	29	•••	62	-62	14	DG	•••	6	330	14.01	24	•••	-39	-26	18	DC-F	•••	
359	(12.39)	(48)	•••	11	-10	3	M+DB	•••	1	374	14.02	50	•••	-20	-9	25	DXP	•••	
100	15.26	131	117	84	-111	8	DK	-0.24		128	12.30	22	•••	38	40	-14	DA	•••	
102	10.56	36	27	34	-30	11	DA	-0.64		129	12.09	63	82	-2	18	-37	DXP	+0.58	
103	11.16	37	•••	34	1	-8	DA	•••		375	13.89	71	84	-14	-3	-7	DC	+0.39	
106	13.60	51	48	58	-56	15	DWK	-0.14		130	12.23	100	98	-5	8	0	DWk	-0.04	
392	13.42	25	•••	19	-36	17	DC	•••		331	10.14	10	•••	25	22	-62	DA	•••	
272	11.90	16	•••	53	-67	16	DB	•••		133	11.20	22	•••	-34	-8	-25	DB	•••	
326	10.95	8	•••	133	-75	54	DA	•••		394	12.08	25	22	12	15	DA	•••		
361	12.18	11	•••	-31	-9	-3	DC	•••		395	11.64	11	•••	61	13	-14	DA	•••	
362	13.91	24	•••	39	-40	22	DF-C	•••		136	(12.24)	(24)	•••	-10	-8	-11	VDAE	•••	5,7
363	(10.98)	(9)	•••	62	-14	7	K+DA	•••	1	376	11.07	9	•••	-137	-6	-19	DA	•••	
111	11.85	18	(3)	62	-229	52	DA	•••		332	10.97	15	•••	-46	8	-12	DA	•••	
297	10.45	11	•••	32	-50	23	DA	•••		333	(11.16)	(19)	•••	17	7	4	DXP	•••	4,6
393	11.38	21	•••	60	-38	9	DB	•••		396	12.43	21	•••	32	4	-11	DA	•••	
364	12.44	35	•••	-5	-7	8	DA	•••		397	10.08	22	•••	29	6	-13	DA	•••	
112	12.78	20	(12)	-26	-61	49	DA	-1.11		139	10.64	68	66	-45	-19	0	DA	-0.07	
185	11.18	29	•••	-7	-25	-7	DA	•••		202	15.73	64	64	32	-11	-53	DC	0.00	
365	13.08	28	•••	-26	-1	3	DA	•••		398	12.15	19	•••	36	7	-3	DC	•••	
262	12.48	31	28	-73	-19	-10	DC	-0.17		154	12.87	22	•••	-61	-39	-12	DA-F	•••	
377	13.83	31	25	-38	-22	-14	DWK	-0.46		155	12.37	41	50	55	-13	-22	DA	+0.46	
334	12.01	17	(15)	31	-1	-48	DC	-0.24		283	14.48	61	49	92	-23	-33	DA-F	-0.49	
399	10.17	26	•••	18	0	-18	DO?	•••	6,8	178	13.85	30	•••	79	-28	-41	DA-F	•••	
400	11.21	10	•••	66	-15	-8	DA	•••		403	10.56	9	•••	76	-22	-12	DA	•••	
378	10.97	55	•••	7	-2	22	DA	•••		404	11.92	14	•••	-34	8	-39	DA	•••	
143	11.48	23	•••	68	-7	-12	DA	+0.46		303	10.54	15	•••	-22	10	4	DA	•••	
144	11.19	50	45	-16	-14	-28	DA	-0.25		380	14.41	30	•••	-2	-24	-37	DWK	•••	
145	11.61	24	21	58	2	-47	DB	+0.22		335	12.40	29	•••	-11	-4	-5	DC	•••	
148	12.98	90	74	-32	-15	-41	DC	-0.41		159	11.65	54	71	-49	-3	-1	V2DA	+0.59	5
149	11.21	19	(11)	32	-38	-56	DB	+0.10	2	336	(12.16)	(65)	•••	•••	•••	•••	VDA	•••	
401	11.70	19	•••	35	3	9	DA	•••		162	11.70	58	56	-22	7	0	DA	-0.06	
402	10.73	13	•••	23	-3	-16	DA	•••		304	9.66	11	•••	•••	•••	•••	DWk	•••	
302	13.31	34	•••	57	17	2	DA-F	•••		405	12.05	16	•••	106	-32	-11	DA	•••	
379	11.92	10	•••	-128	28	-34	DC	•••											

NOTES: 1 - Composite spectrum

2 - Old trigonometric parallax

3 - Not degenerate

4 - Lines affect color

5 - Probably old nova

6 - Important

7 - Possible binary

8 - Possibly Dawk, hot or marginal helium star

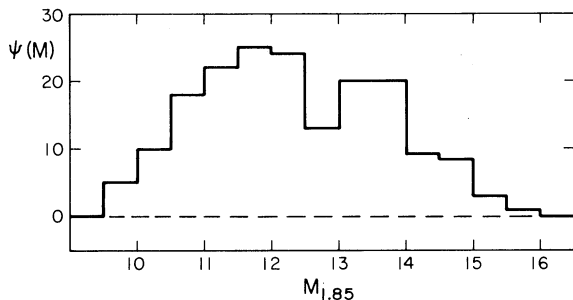


FIG. 6. The luminosities,  $M_{1.85}$ , of 178 degenerate stars with MC scans provide a histogram of the observed frequency function  $\psi(M)$ ,  $N(M+0.25)-N(M-0.25)$  uncorrected for volume of space. In spite of the greater distances over which they are visible, very hot, luminous blue degenerates are rare. The discovery probability of yellow degenerates ( $T < 7000^{\circ}\text{K}$ ) is low, and in spite of extensive search, few are yet known.

location of the least-squares fit to the parallax stars? Given the large range in composition we expect differential line or band blocking to affect the colors. Since the first-order effect in Figs. 3 and 4, the Balmer jump, involves the H/He ratio, we will not try and explain those relations.

It is possible to use a coarse network of presently available model atmospheres to predict the  $G-R$ ,  $G-I$  colors for an assumed  $T_{\text{eff}}$ . The horizontal axes of the figures can then be labeled by  $T_{\text{eff}}$ ; if we assume a radius we obtain the luminosity, i.e.,  $M_{\text{bol}}$ , and need only the bolometric correction to obtain  $M_{1.85}$ . In particular, model atmospheres often give fluxes normalized as  $F_{\nu}/F(1.85)$ , and the absolute value of the flux,  $F(1.85)$ , making the bolometric correction simple. The stars in these figures cover a range of at least  $5000-50\,000^{\circ}\text{K}$ ; at the low  $T_{\text{eff}}$  end only few and uncertain models exist; at the high  $T_{\text{eff}}$  end, the colors cease to vary and  $T_{\text{eff}}$  is poorly determined. For the degree of precision here necessary, I could use Shipman's (1972) models (for DO, DB, and DA) from his thesis, which cover a wide range of  $T_{\text{eff}}$ , and also some cool unpublished models (1976). Comparison with models in the  $7000-12\,000^{\circ}\text{K}$  range by Wehrse (1975) shows general agreement except near  $10\,000^{\circ}\text{K}$ , where a mean value of the deduced color was taken. More careful study of the details of the color- $T_{\text{eff}}$  relation will be required when the entire scan, rather than a few monochromatic magnitudes are fitted. The luminosity of a blackbody at  $T_4$  (in units of  $10\,000^{\circ}\text{K}$ ) and radius  $R_2$  in units of  $10^{-2} R_{\odot}$  is

$$L = 3.451 \times 10^{30} T_4^4 R_2^2. \quad (2)$$

Adopt  $M_{\text{bol}}(\odot) = +4.67$ ,  $L_{\odot} = 3.82 \times 10^{33} \text{ erg sec}^{-1}$ ,  $T(\odot) = 0.577$ ,

$$M_{\text{bol}} = -\frac{5}{2} \log_{10} \frac{L}{L_{\odot}} + 4.67 \\ = 12.28 - 10 \log T_4 - 5 \log R_2. \quad (3)$$

The  $M_{\text{bol}}$  values are given in Table VI, for  $R_2 = 1.2$ , a value which makes the average residual zero. The  $G-I$

and the bolometric corrections, B.C., from Shipman's models (which he kindly provided) are also given in Table VI. This permits us to compute  $M_{1.85}(\text{model})$ , which are compared with  $M_{1.85}(\text{cubic})$ , the value obtained when the  $G-I$  computed from the model is inserted in the cubic equation given in Table IV, and fitted to the observations in Fig. 1. The differences  $O-C$ ,  $M_{1.85}(\text{cubic}) - M_{1.85}(\text{model})$  are given in the last column. They are small and do not show any large trend over a tenfold change in  $T_4$ , i.e., a change of  $10^4$  in luminosity. The mean deviation is  $\pm 0.21$  mag, surprisingly good, since  $G-I$  colors predicted from Shipman and Wehrse sometimes differ by 0.10 mag. The radius may not be completely determined, depending on the B.C. Comparison is possible with ATLAS models by Kurucz, Peytremann, and Avrett (1974) for main-sequence stars ( $\log g = 4.5$ ). Their absolute calibration through the solar flux is quite different, and their minimum B.C. is near zero at  $8000^{\circ}\text{K}$ ; Shipman's minimum B.C. is 0.24 for a cool model in which  $H_2$  opacity dominates. However, decreasing the B.C. by 0.20 mag changes the mean radius only to  $1.09 \times 10^{-2} R_{\odot}$ . If we repeat this process using  $G-R$  colors, the result is less satisfactory, probably because of errors in the colors of models. The fit is poor at high  $T$  when the  $G-R$  rapidly approaches the Rayleigh-Jeans-law limit. In resumé, the parallax data define a relatively narrow, single sequence in suitable color-magnitude plots. Even at the extremes of temperature, the degenerate stars can be understood as a cooling sequence of constant mean radius. The very hot, luminous stars like HZ 43 and G191B2B fit this cooling sequence. The young ( $< 3 \times 10^7$  yr) DA, EG 25 (LB 1497) in the Pleiades (Luyten and Herbig 1960), has its membership confirmed by Jones' (1973) proper motion study. Its photometry lead to predicted  $M_{1.85} = 10.41$ , while its cluster membership gives  $M = 11.00$ , well within the scatter observed in the parallax sample. Thus neither high bolometric luminosity nor youth cause large deviations from the mean radius. The present parallax sample does not include hot subdwarfs. Blanketing vectors may differ for different composition, without

TABLE VI. Prediction of  $M_{1.85}$  for degenerate stars hydrogen models,  $\log g = 8$ ,  $R = 1.2 \times 10^{-2} R_{\odot}$ .

$T_4$	From models			$M_{1.85}$	$M_{1.85}$	$O-C$
	$M_{\text{bol}}$	B.C.	$G-I$	model	cubic	
0.5	14.90	0.34	0.90	15.24	14.92	-0.32
0.6	14.11	0.24	0.40	14.35	14.18	-0.17
0.7	13.44	0.30	0.14	13.74	13.71	-0.03
0.8	12.86	0.36	0.00	13.22	13.42	+0.20
0.9	12.35	0.42	-0.18	12.77	12.99	+0.22
1.0	11.89	0.48	-0.34	12.37	12.55	+0.18
1.2	11.10	0.77	-0.57	11.87	11.81	-0.06
1.4	10.43	1.16	-0.71	11.59	11.28	-0.31
2.0	8.88	2.09	-0.85	10.97	10.69	-0.28
2.8	7.42	2.95	-0.94	10.37	10.27	-0.10
3.7	6.15	3.52	-1.04	9.67	9.78	+0.11
5.0	4.90	4.49	-1.08	9.39	9.57	+0.18

substantially affecting this agreement, as long as we do not use colors sensitive to the Balmer jump.

#### IV. DATA ON LUMINOSITIES, MOTIONS, PARALLAXES FROM MC COLORS

We have used the data of Table II without full description. The data are star name; 1950 position; proper motion (MU) in seconds of arc/yr and position angle (TH); Lowell color (LC); reduced proper motion  $H = m1.85 + 5 \log \mu$ ; quality of MC scan ( $Q$ ); the number 1 under  $P$  if a parallax exists;  $I$  to  $U$ , monochromatic magnitudes on the Oke  $AB$  scale;  $R^* - I^*$  color; M1 and M2 line indices described below; type of spectrum; EG or Gr number; transverse motion  $T$ , in kilometers/sec from the photometry and REF described below. In Table III the colors from Table II are given explicitly for stars of known parallax. EG or Gr numbers, used in Tables II, III, and V permit reference from table to table, and are, of course, not in serial order. In classification of type, the appearance of the scan was used, i.e., visibility of hydrogen, helium, or metallic lines. To quantify the latter, two line indices were developed for main-sequence and degenerate stars. They measure in hundredths of a magnitude the Mg I and MgH features (M1) and the Ca II and H $\zeta$  (M2); they require special measures at  $1/\lambda = 1.94$  ( $\lambda 5155$ ) and  $2.58$  ( $\lambda 3876$ ):

$$M1 = [1.94] - 0.5([2.12] + [1.85]), \quad (4)$$

$$M2 = [2.58] - 0.5([2.80] + [2.35]). \quad (5)$$

The MC has lower resolution than the prime-focus spectra I used, and classification is rougher, since features below 3-Å equivalent width cannot be seen. Thus weak-hydrogen-lined stars (formerly DA<sub>W</sub>k or DA<sub>S</sub>) may be classified as DC and weak Ca II lined stars (DA, F, or DF) may also be called DC. If cool degenerate stars had normal metal abundances the Mg features would produce positive M1. In fact, abundances are so low that M1 is near zero except for the strange DG star (M1=48) Gr 391 (G165-7). The M2 index is positive ( $\approx 20$ ) for DA stars because of H $\zeta$  but is large (44 and 89) for DG stars (EG 5, 391) which have no Balmer lines. Cool degenerates have slightly positive M2 even when  $\lambda 3933$  is not seen on the scans. Color-color and line-color relations will be studied elsewhere, but the data in Table II should suffice to justify classification as degenerate, based on the MC.

From the colors in Table II the three polynomials fitted above to the parallax stars predict  $M_V$  for 178 stars. These and the resulting  $T$  are computed, used in Tables II and V to compute parallaxes (in  $0.^{\circ}001$ )  $P$  (ptm) and also space motions in kilometers/sec,  $U$  (positive away from the galactic center),  $V$  (in the direction of galactic rotation), and  $W$  (towards the north galactic pole). Table V also includes trigonometric parallaxes and notes. If a sdB or sdG star has been

erroneously called a degenerate, its  $U$ ,  $V$ ,  $W$  will be outstandingly small. Conversely, if a degenerate star is not recognized, its  $U$ ,  $V$ ,  $W$  will be too large. While some of the latter stars have MC scans, they are mostly not in this list; an example of what Eggen calls RSL (red subluminous) is EG 320 (LTT 2437), for which I predict  $0.^{\circ}111$  parallax, if it is degenerate, and  $T = 11$  km sec $^{-1}$ . If it is an ultra-weak-lined sdG,  $M_V = 5.4$  and  $T = 772$  km sec $^{-1}$ , resulting in  $W = +724$  km sec $^{-1}$ , i.e., far above the escape velocity.

Some stars previously called degenerate, i.e., with EG or Gr numbers are not degenerate, or are in composite systems for which MC colorimetry cannot be used, i.e., EG 309, 20, 21b, 27, 38, 388, 91, 359, 363, 136, 336.

Inspection of Table V shows that the photometric parallax has  $\sigma[P(\text{ptm}) - P(\text{trig})] = \pm 0.^{\circ}014$  [excluding EG 11 for which  $P(\text{trig})$  must be incorrect]. The effect of line blanketing on colors is quite large for some stars, for example, EG 5 (DG), EG 24, 182 ( $\lambda 4670$ ), EG 100 (DK), EG 372 (DXP). Omitting these and some with poor  $P(\text{trig})$ , EG 340, 111, 196, the dispersion  $\sigma[P(\text{ptm}) - P(\text{trig})] = \pm 0.010$ , about  $\pm 0.007$  in each source, which seems reasonable. For prediction of objects worth the effort of trigonometric measurement, Table V has reasonably small error.

A few stars deserve remark. The critical DB stars are, unfortunately, likely to have small  $P$ , the largest being  $0.^{\circ}024$ . Several magnetic polarized stars DP have unmeasured but large parallaxes; EG 333 has so large a blanketing that its  $P$  might be as large as  $0.^{\circ}045$ . There are 18 stars with  $M_V > 13.5$  which have no  $P(\text{trig})$ ; their  $\langle P(\text{ptm}) \rangle = 0.^{\circ}048$  and they are mostly cooler than 7000°K.

The space motions, either as  $T$  or  $U$ ,  $V$ ,  $W$  show a remarkably low-velocity characteristic. The median  $T$  is 48 km sec $^{-1}$ , and less than 10% exceed 100 km sec $^{-1}$ ; 3% are halo-type motions ( $T > 150$  km sec $^{-1}$ ). Analysis of the  $U$ ,  $V$ ,  $W$  gives

$$\langle U \rangle = +11 \pm 3, \quad \sigma(U) = \pm 43,$$

$$\langle V \rangle = -23 \pm 3, \quad \sigma(V) = \pm 36,$$

$$\langle W \rangle = -5 \pm 2, \quad \sigma(W) = \pm 26.$$

With reversed sign these give a solar motion almost identical with that of solar-type main-sequence stars, as given by Delhaye (1965), although the dispersions are appreciably larger. According to Delhaye an empirical linear relation exists between  $\sigma^2(\Pi)$  and  $\Theta$ ; the white dwarfs fall on that relation, suggesting a rather uniform density. The  $\sigma(W)$  would permit oscillation up to 400 pc. More realistic examination of the distribution of  $U$ ,  $V$ ,  $W$  suggests that the white dwarfs belong to both the young and old disk, but also, very rarely to the halo population. Take the critical velocity coordinate  $V$ ; two stars have  $V > +40$  km sec $^{-1}$ , and two have  $V < -200$  km sec $^{-1}$ .  $|U|$  exceeds 100 km sec $^{-1}$  for seven stars;  $|W| > 60$  km sec $^{-1}$  for five stars, which

would carry them nearly to 1 kpc from the plane. Thus, in spite of the selection favoring high-velocity stars and in spite of the very long cooling life times for degenerate stars, the halo population fraction in this sample is estimated to be at most 2% or 3%.

#### ACKNOWLEDGMENTS

I am grateful to Todd Boroson for programming the preparation of computer-generated tables, to Grace Knox for preparation of the punched cards from the original data, and to Marilynne Rice for her preparation of the manuscript.

#### REFERENCES

- Delhaye, J. (1965). *Galactic Structure*, edited by A. Blaauw and M. Schmidt (Univ. Chicago P., Chicago).
- Eggen, O. J., and Greenstein, J. L. (1965). *Astrophys. J.* **141**, 83.
- Giclas, H. L., Burnham, R., Jr., and Thomas, N. G. (1962). Lowell Obs. Bull. No. 118.
- Giclas, H. L., Burnham, R., Jr., and Thomas, N. G. (1971). *The G Numbered Stars* (Lowell Obs., Flagstaff).
- Gliese, W. (1969). *Catalogue of Nearby Stars* (G. Braun, Karlsruhe).
- Greenstein, J. L. (1974). *Astrophys. J. Lett.* **189**, L131.
- Greenstein, J. L. (1975). *Astrophys. J. Lett.* **196**, L117.
- Harrington, R. S., Dahn, C. C., Behall, A. L., Priser, J. B., Christy, J. W., Riepe, B. Y., Ables, H. D., Guetter, H. H., Hewitt, A. V., and Walker, R. L. (1975). *Publ. U. S. Naval Obs.* **24**, Pt. 1.
- Hearn, D. R., Richardson, J. A., Bradt, H. V. D., Clark, G. W., Lewin, W. H. G., Mayer, W. F., McClintock, J. E., Primini, F. A., and Rappaport, S. A. (1976). *Astrophys. J. Lett.* **203**, L21.
- Jones, B. F. (1973). *Astron. Astrophys. Suppl.* **9**, 313.
- Kurucz, R. L., Peytremann, E., and Avrett, E. H. (1974). *Blanketed Model Atmospheres for Early Type Stars* (Smithsonian Inst., Washington, DC).
- Luyten, W. J. (1949). *Astrophys. J.* **109**, 528.
- Luyten, W. J., and Herbig, G. (1960). Harvard Announcement Card No. 1474.
- Margon, B., Malina, R., Bowyer, S., Cruddace, R., and Lampton, M. (1976a) *Astrophys. J. Lett.* **203**, L25.
- Margon, B., Liebert, J., Gatewood, G., Lampton, M., Spinrad, H., and Bowyer, S. (1976b). *Astrophys. J.* To be published.
- Oke, J. B. (1974). *Astrophys. J. Suppl.* **27**, 21.
- Oke, J. B., and Schild, R. E. (1970). *Astrophys. J.* **161**, 1015.
- Riddle, R. K. (1970). *Publ. U. S. Naval Obs.* **20**, Pt. 3.
- Routly, P. (1972). *Publ. U. S. Naval Obs.* **20**, Pt. 6.
- Shipman, H. L. (1972). *Astrophys. J.* **177**, 723; also Ph.D. thesis, California Institute of Technology.
- Shipman, H. L. (1976). In preparation.
- van Altena, W. J. (1969). *Astron. J.* **74**, 2.
- van Altena, W. J. (1971). *Astron. J.* **76**, 932.
- van Altena, W. J., and Stone, R. C. (1973a). *Astron. J.* **78**, 781.
- van Altena, W. J., and Vilkki, E. U. (1973b). *Astron. J.* **78**, 201.
- van Altena, W. J., and Vilkki, E. U. (1975). *Astron. J.* **80**, 647.
- Wehrse, R. (1975). *Astron. Astrophys.* **39**, 169.